Robust var unit control strategies for damping of power system oscillations
by James Robert Smith

A thesis submitted in partial fulfillment of the requirements for the degree of Doctor of Philosophy in Electrical Engineering
Montana State University

Abstract:
This thesis is concerned with the development of var unit control strategies to improve the damping of electromechanical oscillations (0.1 to 2.0 hertz) which commonly occur in power systems. The objective is to use network information, locally available at the var unit bus, to produce a signal which determines the appropriate time-varying susceptance of the var unit.

Two strategies, one nonadaptive and one adaptive, are developed. The nonadaptive control strategy is based on a computer generated linearization of the nonlinear power system model. A fixed controller design is then obtained using eigenvalue analysis. The adaptive control strategy is based on real-time identification of reduced-order models of the system. An adaptive, linear quadratic, optimal controller is then formulated which determines the var unit susceptance values needed to quickly reduce system oscillations. The effectiveness of each of these control strategies is tested by computer simulation of a nine-bus power system. A detailed explanation of the methods used to simulate power system dynamics are also presented.

The simulation results illustrate the potential usefulness of applying these types of controllers to dampen oscillations of large inter-connected power networks. The robust character of these controllers is also illustrated.

ROBUST VAR UNIT CONTROL STRATEGIES FOR DAMPING

OF POWER SYSTEM OSCILLATIONS

by

James Robert Smith

A thesis submitted in partial fulfillment
of the requirements for the degree

of

Doctor of Philosophy

in

Electrical Engineering

MONTANA STATE UNIVERSITY
Bozeman, Montana

July 1988

ii

APPROVAL

of a thesis submitted by

James Robert Smith

This thesis has been read by each member of the thesis committee
and has been found to be satisfactory regarding content, English usage,
format, citations, bibliographic style, and consistency, and is ready
for submission to the College of Graduate Studies.

_____7/22/88_____
Date

_____
Chairperson, Graduate Committee

Approved for the Major Department

_____7/22/88_____
Date

_____
Head, Major Department

Approved for the College of Graduate Studies

_____August 1, 1988_____
Date

_____
Graduate Dean

STATEMENT OF PERMISSION TO USE

In presenting this thesis in partial fulfillment of the requirements for a doctoral degree at Montana State University, I agree that the Library shall make it available to borrowers under rules of the Library. I further agree that copying of this thesis is allowable only for scholarly purposes, consistent with "fair use" as prescribed in the U.S. Copyright Law. Requests for extensive copying or reproduction of this thesis should be referred to University Microfilms International, 300 North Zeeb Road, Ann Arbor, Michigan 48106, to whom I have granted "the exclusive right to reproduce and distribute copies of the dissertation in and from microfilm and the right to reproduce and distribute by abstract in any format."

Signature _James R. Smith_

Date _Aug 1, 1988_

ACKNOWLEDGEMENTS

TABLE OF CONTENTS

TABLE OF CONTENTS--Continued

LIST OF TABLES

LIST OF FIGURES

LIST OF FIGURES--<u>Continued</u>

LIST OF FIGURES--<u>Continued</u>

ABSTRACT

This thesis is concerned with the development of var unit control strategies to improve the damping of electromechanical oscillations (0.1 to 2.0 hertz) which commonly occur in power systems. The objective is to use network information, locally available at the var unit bus, to produce a signal which determines the appropriate time-varying susceptance of the var unit.

Two strategies, one nonadaptive and one adaptive, are developed. The nonadaptive control strategy is based on a computer generated linearization of the nonlinear power system model. A fixed controller design is then obtained using eigenvalue analysis. The adaptive control strategy is based on real-time identification of reduced-order models of the system. An adaptive, linear quadratic, optimal controller is then formulated which determines the var unit susceptance values needed to quickly reduce system oscillations. The effectiveness of each of these control strategies is tested by computer simulation of a nine-bus power system. A detailed explanation of the methods used to simulate power system dynamics are also presented.

The simulation results illustrate the potential usefulness of applying these types of controllers to dampen oscillations of large inter-connected power networks. The robust character of these controllers is also illustrated.

CHAPTER 1

INTRODUCTION

Problem Description and Background

This thesis is concerned with the development of control strategies which can be applied to a static var compensator (SVC) in order to enhance the damping of electromechanical oscillations which occur among generators in power networks. These oscillations generally occur in the frequency range from around 0.1 to around 1.5 hertz. Consideration of different strategies has been limited to those control strategies which will require only local information readily available at the bus where the var unit is located. This requirement means that effective control action will not depend on the measurement and communication of information from widely dispersed parts of the network. The benefit here is that the controller reliability will not be subject to the reliability of the communication system. This is a concern in power systems since the same environmental factors which cause disturbances to power systems may also cause disturbances to communication systems.

A static var compensator is one of several devices that can be utilized to enhance damping in a power system. Other devices to accomplish the same goal include power system stabilizer (PSS) control on exciters, control of series compensators, and control of high voltage DC (HVDC) converter systems. Static var compensators have an

advantage over power system stabilizers in that they can be centrally located in the power network in order to obtain maximum effectiveness. Also they may be more feasible to use for a utility company that is primarily a power transmission company and not a power generation company. Static var compensators are often installed primarily for voltage support in a network, and controlling the device to improve system damping as a secondary function adds additional benefit. High voltage DC systems have many of the same advantages as static var compensators for improving system dynamics. A disadvantage of using high voltage DC converter control is that a primary need of enhanced system damping may be when the DC intertie is lost. In this case the disturbance itself eliminates the HVDC system from being part of the solution to the problem. The control of series compensation devices has not been considered here since the continuous control of such devices is very new and their reliability and economic feasibility in the power system environment has not been tested. It should be noted however, that the control strategies developed here and applied to static var compensators can just as well be applied to these other devices.

The need to improve damping in power systems networks has been growing over the years [1]. Poorly damped oscillations have been noticed in power systems in many parts of the world. The major factor contributing to these oscillations is often the use of long transmission lines carrying large power flows from one area of a system to another. In some cases this situation is due to the development of generating facilities that are located in remote areas from the major load centers. Undamped or poorly damped oscillations are often the

limiting factor encountered in determining how much power can be transported from one area of a system to another. This situation may arise when a utility faces the problem of meeting growing load demands on an existing system where expanding transmission capacity is limited by increasing restrictions and costs of new transmission lines. Maximizing power transfers over existing lines is a major goal of many utilities, and system damping is often the obstacle to overcome. Damping problems are also sometimes attributed to peculiar load dynamics or to the widespread use of fast acting generator excitation systems. These excitation systems are important to maintain system integrity in the event of sudden disturbances. Some utility companies report that their transient stability studies of projected system operating conditions indicate that the poor damping problem will get worse in the years ahead [2].

There are several problems associated with sustained or poorly damped oscillations in power system networks. The presence of the oscillations themselves indicates a lack of stability in the system operating point which may potentially worsen causing the system to be unstable. There is also the possibility that a second disturbance occurring during the oscillatory period may cause the system to go unstable and separate, whereas the same disturbance occurring in a more settled situation would not. Large oscillations in voltage and power flows threaten the system integrity by causing damage to equipment belonging to both the utility and the customer. There is also the danger of undamped oscillations initiating or aggravating a cascading outage.

Power systems in general present a challenging problem for designers of control systems who want to try to modify the power system dynamics. There are four characteristics of power systems which need special attention. First, a power system is a nonlinear system. Since there are very few generally applicable control techniques for nonlinear systems, controller design for a power system usually involves a linearized representation of the nonlinear system. Second, the power system is a time-varying system. Generally there is a slow continuous change in the operating point of the system with daily as well as yearly cyclical patterns being present. This means that the dynamics of the system are constantly changing also. These changes are usually slow and occur over periods of hours but occasionally the system dynamics can undergo large changes in a period of seconds or less. This time-varying nature of the system is often neglected in designing controllers for power systems with the result that the controllers are usually only effective for certain operating conditions and may actually be detrimental to system dynamics under other operating conditions. Third, a power system is usually a very high-order system. Even a small utility is often interconnected with other utilities so that a thorough representation of the system will involve hundreds or even thousands of buses. This characteristic of power systems causes problems for many standard approaches to controller design. Fourth, power systems are multivariable systems with numerous inputs and outputs scattered over long distances so that coordination of controllers in different parts of the system can be difficult.

In this thesis two approaches to controller design are presented. Both of these approaches attempt to deal with all four characteristics

mentioned above with special emphasis on the time-varying aspect of the system. The first approach utilizes a linearized system representation and eigenvalue analysis to design a controller which meets the needs of the system over a wide range of operating points. The second approach utilizes an adaptive controller with on-line identification of a reduced-order transfer function of the power system.

Power System Damping

A simplified power system model having n generators will have n-1 modes or frequencies of oscillation [3]. These are often referred to as natural frequencies of oscillation. Normally in a power system all these modes will be positively damped. Occasionally some of these modes may have only slight positive damping in which case oscillations will persist for a long time after a disturbance before they die out. If a mode becomes negatively damped then oscillations will arise spontaneously. An oscillation or mode that is poorly damped may involve only one or two machines or it may involve large groups of machines. In general oscillations involving only a few machines occur in the frequency range from 1 to 2 hertz. Oscillations involving large groups of machines generally occur at frequencies below 1 hertz [3]. Oscillations involving large numbers of machines are usually difficult to analyze because of the amount of detail required in the computer representation to reproduce the oscillations in simulations. There are a few papers which have appeared in the literature which report on

efforts to analyze the causes and factors affecting the occurrence of certain modes which have been recorded in power systems [4], [5] and [6].

There are two basic approaches to understanding power system damping which often are mentioned in the literature. One approach is based on the concepts of synchronizing and damping torques which were developed by deMello and Concordia [7] in order to gain insight into the design of power system stabilizers. The second involves the concepts of eigenvalue analysis which have been utilized by many authors for both the analysis of factors causing poor damping and the design of controllers to improve system damping. While the synchronizing and damping torques concept is based on a one-machine infinite-bus system it has proven very insightful and useful even in multimachine systems and has been used with very good success in the design of power system stabilizers. Many authors have been attempting to extend the use of these concepts for designing other types of damping control also. Recently eigenvalue analysis programs have been developed which are capable of finding eigenvalues of very large power systems [8] and [9]. Eigenvalue analysis has been used to design stabilizing controllers for many different types of control approaches including, HVDC converters, SVC systems and power system stabilizers.

The concept of damping torques and synchronizing torques was developed based on the one-machine infinite-bus power system. These concepts illustrate how machine stability is affected by the excitation system as well as by network parameters and operating conditions. Equations (1.1) and (1.2) below are the swing equations written in state equation form where M is machine inertia constant, ω is the rotor

slip speed in per unit, δ is the rotor angle in radians, T_m and T_e are the mechanical input torque and electrical output torque respectively, and D is the damping coefficient.

$$\dot{\omega} = \frac{1}{M} (T_m - T_e - \omega D) \tag{1.1}$$

$$\dot{\delta} = 377\omega \tag{1.2}$$

If we define the synchronizing torque coefficient K_1, as $K_1 = \Delta T_e / \Delta \delta$, then a linearized small perturbation representation of these equations can be put into a block diagram as in Figure 1.
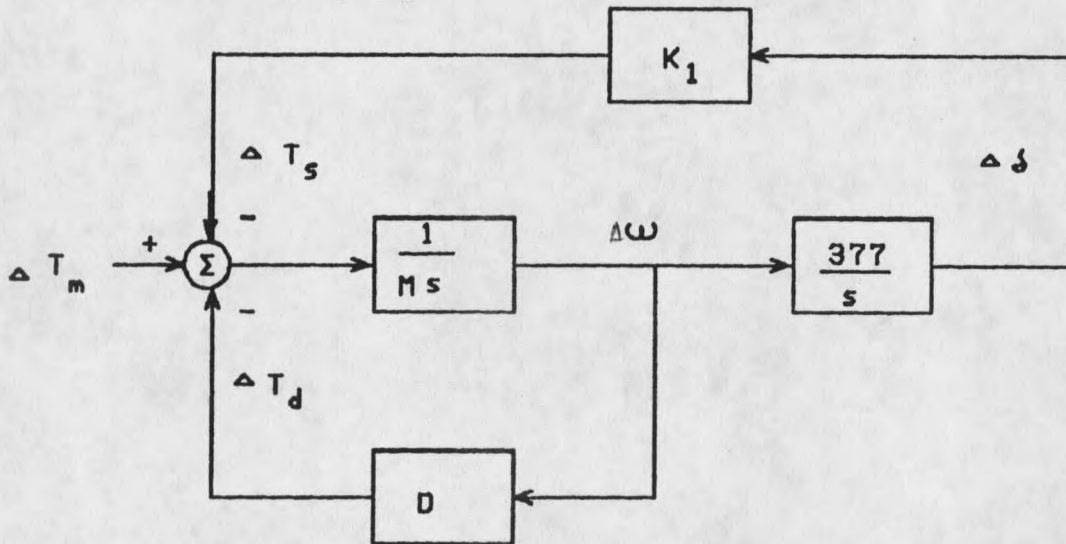
Figure 1. A diagram of linearized machine torque relations.

In this diagram a change in the mechanical torque input of the machine ΔT_m is counteracted by two opposing torques. ΔT_s is referred to as the synchronizing torque, and ΔT_d is referred to as the damping

torque. These two torque components have a 90 degree phase shift between them. Any torque in phase with rotor velocity is referred to as a damping torque and those in phase with rotor angle are synchronizing torques. An arbitrary mechanical torque input will require a combination of both counteracting torques in order to reach a steady-state operating point again. The synchronizing torque acts to prevent the machine from losing synchronism with the rest of the network and is strongly dependent on network parameters as well as the machine excitation system. The damping torque is affected by factors such as rotor amortisseur windings and the excitation system. The torque-angle characteristic equation of this block diagram is

$$s^2 + (D/M)s + (K_1 377/M) = 0 \qquad\qquad (1.3)$$

which has an undamped natural frequency of $\omega_n = \sqrt{377K_1/M}$ and a damping ratio of $\zeta = 0.5D/\sqrt{377K_1 M}$. With these ideas established it can be shown, [7], that under certain commonly encountered conditions the voltage regulator can have a beneficial effect on synchronizing torques while simultaneously reducing the damping torque of the machine.

Eigenvalue techniques have been used in some cases to analyze the factors contributing to well documented oscillations that have occurred in power systems. The Ludington Pumped Storage Plant located in Michigan experienced undamped oscillations early in the morning of December 28,1973. System conditions and operating parameters at the time were well documented [4]. The plant contains six reversible generator/pump units. Water is pumped up to a reservior and later released to generate electricity with an electrical efficiency of 70%. The oscillations occurred at a frequency of about 0.77 hertz when the

sixth unit was put on line to start pumping. The authors report that eigenvalue analysis indicated that a lack of damping of normal mechanical oscillations is what was causing the sustained oscillations.

The factors affecting the damping were found to include the external system equivalent reactance. Higher values of external equivalent reactance due to transmission lines being out of service caused negative damping of the system. Increasing the pumping power being consumed at the plant also contributed to negative damping. Damping was found to be improved slightly by increasing voltage levels in the system. The most significant factors related to changes in damping were found to be changes in excitation system parameters. The authors also report that neglecting amortisseur windings on the machines had only a slight effect on eigenvalues while neglecting stator resistance in the machine models had no significant effect on eigenvalues.

It is interesting to note that these oscillations occurred in a tightly connected and lightly loaded transmissions system. Damping in this study was found to be most strongly affected by machine loading and excitation system parameter settings.

A detailed analysis of an instability that occurred in Illinois at the Powerton Generating Station is described in [5]. This situation, in which a large generator is being operated at the end of a long transmission line, is well known to have stability and damping problems. An oscillation frequency of about 1.0 hertz was observed to occur whenever the generation from the facility exceeded a certain limit. It was noticed that the oscillations could always be eliminated by reducing the power output or by disconnecting the automatic voltage

regulator. After further investigation it was established that adjustment of excitation system parameters could also restore stability. All of these observations were reproduced by simulation and verified by eigenvalue analysis. It was found that the largest effect on critical eigenvalues came from forward loop gain and the feedback gain on the excitation system. Stability could also be affected in this case by raising the terminal voltage.

Review of Literature on SVC Control for System Damping

This section will review some controller designs for SVC's which have appeared in the literature for the purpose of improving system damping and stability. Ohyama,et al., [10] have proposed a method of SVC control to enhance system damping using a so-called "reset filter". The purpose of the reset filter is to allow SVC utilization for steady-state voltage control along with damping control. The controller is designed for a one-machine infinite-bus system. Using this system the authors derive expressions relating the SVC reactance to the machine synchronizing torque coefficient. A relationship is also derived relating SVC setting to machine oscillation frequency. By increasing the oscillating frequency it is argued that the machine damping torque is increased slightly. An eigenvalue study on a large system shows that controlling the SVC increases system damping of the main mode but no details of the particular control system are provided. The reset filter basically prevents the damping portion of the SVC control from reacting to voltage level adjustments of the SVC.

Hammad [11],[12], has given a review of some SVC control techniques as well as proposing an optimal control strategy. The system proposed here has damping control as a separate loop from voltage regulation control. The damping control proposed is of the "bang-bang" type. Arguments are presented, based on a one-machine infinite-bus system, that pure voltage control alone will provide machine synchronizing torque but not damping torque. It is then shown that SVC control based on rotor speed or change in power will provide damping. For velocity feedback, the increased synchronizing torque is proportional to the gain of the controller which then leads to a justification for the use of bang-bang control. The author uses Pontryagin's maximum principle to derive an optimal bang-bang control strategy for the one-machine case.

Olwegard, et al., [13] also have looked at the application of SVC's to enhance system damping. The authors are interested in the Nordel power system which covers Sweden, Finland, Norway, and Denmark. Damping has been a factor of critical concern for this system since the 1960's. The authors use a one-machine system to develop a simple scheme of switching in SVC reactance based on power transfer fluctuations. The control scheme comes into effect only when power oscillations exceed a certain threshold value but also are less than a certain maximum value. Computer simulations of the Nordel system indicate undamped oscillations will occur when a certain tie-line is lost which can be stabilized by the SVC control. The application of SVC control enables higher power transfers in the system which translates into an SVC effectiveness measure of so many MW of power transfer increase per MVAR of SVC capability. The authors briefly

discuss the control of thyristor controlled series capacitors but report that a suitable control scheme has not been found. They feel that series capacitors are more readily suited for enhancement of first swing transient stability than is a shunt device.

Hamouda, Iravani, and Hackam [14] have considered coordinating SVC control with PSS control in order to damp machine inertial oscillations as well as torsional shaft oscillations. The main application of the SVC is voltage control with an auxiliary input voltage signal to damp oscillations obtained from generator speed deviation. Their work describes an SVC application for a one-machine system. Their emphasis is mainly on subsynchronous resonance with a reported improvement in system damping of around 3% for some modes.

. Larsen and Chow [15] have given some insights for SVC control applied to both voltage level control and system damping. They report that the transient response of their voltage control loop used in voltage level control has a limit to its speed of response which is determined by the tendency of the loop to undergo oscillations at around 20 hertz. The approach they use toward enhancing system damping is to look at each system mode independently and apply the concepts of synchronizing and damping torques to the machines. For each modal frequency, a diagram is developed representing the effects of the SVC control on synchronizing and damping torques for a machine. Transfer functions are developed relating SVC voltage level to modal speed and angle. The torque components due to the SVC, in phase with modal speed and angle, are identified. Since the torque component in phase with modal speed is usually very small, a supplementary control function is developed to utilize another controller input signal to modulate SVC

voltage to increase this torque component. Three basic system signals are considered as inputs to the damping controller: ac voltage frequency, current or power flow on a tieline, and voltage magnitude. The issues of swing mode controllability and observability for each of these controller inputs is discussed. Because the authors are controlling the voltage level of the SVC as the controller output and using another system signal as the controller input, they have an "inner loop" in their control system where the controller output is affecting the controller input signal without affecting system damping. The gain of this inner loop is an important factor in the selection of a suitable controller input signal. The problem of designing a controller involves minimizing the gain of this inner loop while providing purely positive damping from the controller output. The amount of damping obtained will vary with power system operating condition as will the inner loop sensitivity. The authors note that using active current as the controller input signal has the advantage of low inner loop sensitivity whereas voltage magnitude is dropped from consideration because of high inner loop sensitivity. Both active current and power change sign as a function of operating condition and so the authors report that an adaptive control scheme would be necessary to utilize these signals effectively. Current magnitude is reported as having the best attributes overall as an input signal to the controller. Controller design also has to incorporate washout and high frequency filtering stages to isolate the swing mode of interest. Improved system damping using this control scheme is simulated on two-area and three-area systems. In these simulations each area is represented by an equivalent machine.

Martin [16] proposes an SVC control strategy for combining both voltage control and system damping. In this case the damping signal is an auxiliary input into the SVC regulator. He proposes using only bang-bang type control for system damping with the SVC at either its maximum or minimum reactive power output. Some inputs that are considered are: rate of change of angle between two system areas, rate of change of power on the tieline, and system frequency or machine rotor speed in one of the areas. A three-area system (with each area represented by one equivalent machine) was simulated to test the controller design. The author reports that using rate of change of angle between two areas is not a practical signal and rate of change of power, though easy to measure, was not an effective signal. Frequency of one of the areas proved to be the most effective choice. The final design used frequency of area one with proper filtering to limit the SVC response to the frequencies of interest. The author also develops the performance measure of MW/MVAR which indicates the amount of increased allowable tieline power flow per MVAR of SVC capacity that is required to obtain acceptable system damping.

Adaptive Controllers in Power Systems

The time-varying nature of power system dynamics makes the industry an inviting area for the application of adaptive controllers. Power system dynamics are constantly changing with load levels and generation pattern adjustments both on a daily and seasonal cycle. This characteristic means that a fixed type of controller designed by

conventional means can be expected to perform with high effectiveness during only a small part of its operating time. In some circumstances or operating conditions the fixed controller may actually have adverse effects on system dynamics. An adaptive controller which continually updates or "tunes" itself to the current operating conditions is one way to solve this problem.

Many adaptive controllers for power system applications have been proposed in the literature, but the actual implementation of adaptive controllers in power systems is nonexistent or at least very rare [17]. Most of these proposed applications have been applied to generator excitation systems and load-frequency controllers, with a few proposed for HVDC systems and, until recently, only one for SVC control. This review of adaptive controllers in power systems will be limited to a series of papers on a pole-shifting type of adaptive controller applied to PSS systems and to a brief mention of the one SVC adaptive control strategy. A more thorough review of adaptive control strategies proposed for power systems can be found in [17] or [18]. Background relevant to an enhanced LQ adaptive controller is given in the introductory section of Chapter IV.

Cheng, Malik, and Hope with several other coauthors have written several papers [19], [20], [21], describing a self-tuning adaptive controller based on a pole-shifting strategy and applied to PSS control in order to enhance system damping. The authors have designed their controller using a dual-rate sampling scheme in order to keep the sampling interval small and yet still have enough time to perform the necessary computations between samples. The computations are done using multiple microprocessors. Their controller uses a self-adjusting

pole shifting strategy, which attempts to shift the poles of the controlled system toward the origin of the z plane by a factor α. This factor, α, varies between zero and one to produce a control effort that results in maximum damping of the system oscillations, yet does not exceed controller limits. The controller is basically a feedback compensator which is tuned to shift the poles of the closed-loop system. The desired control law for the machine is obtained as a function of: the system parameter vector obtained from an identifier, a vector containing the present and past system outputs, and a vector of past inputs.

The basic assumption made in this controller and in many self-tuning controllers is that a very high-order system can be modeled as a much lower order system and an effective control law can be calculated based on this low-order model. It is also implied that the essential time-varying parameters of the system can be identified and tracked over periods of time and the control law adjusted to maintain maximum effectiveness. The identifier used by the authors is of the recursive least squares (RLS) type with a varying forgetting factor to enhance its tracking ability.

The authors report that using the pole-shifting adaptive control strategy has the advantages of being applicable to nonminimum phase systems as well as the desirable characteristic of always producing a smooth control action. The parameters of the feedback compensator are found by solving a system of linear equations of size 2n-1 where n is the order of the identified model. It is reported that a third-order model gives good results in their studies and a fifth-order model is impractical for real-time implementation using 8086 microprocessors.

The authors have obtained very promising simulation results using this control scheme. In reference [19] they have tested the method on a one-machine system. In [20] they have demonstrated its effectiveness in a three-machine system which has two lightly damped modes of oscillation. Their latest paper [21] illustrates the effectiveness of having this controller on one, two or all three machines in the system.

It is interesting to note that Wu and Hsu [22] have used the pole shifting method also to adaptively adjust the parameters of a PID controller for a PSS system. They have reported successful simulation results using a second-order identified model. Their controller was tested by simulation on a nine-bus system which is a variation of the same nine bus system to be used later in this thesis.

Other than the adaptive strategies proposed by this author and associates [23], [24], [25], the only adaptive strategy proposed so far for application to an SVC is given in reference [26]. In [26] the SVC is designed to increase damping on a one-machine system. The SVC controller uses machine rotor velocity as the feedback variable, and the gain settings of the PI feedback compensator are adjusted according to a table lookup method by reference to the machine real and reactive power loading. Off-line eigenvalue analysis is used to determine the gain settings for each operating condition and to form the lookup table. The SVC in this system is located at the machine terminal bus and can be used in lieu of a PSS.

Robust Fixed Controllers in Power Systems

It is well accepted that when system conditions are accurately known then successful power system controllers can be designed for those conditions. When damping enhancement is desired for several different operating conditions then controller design techniques are less established and the problem is often categorized as a robustness problem. Robustness is generally regarded as a quality of the controller that enables it to be effective despite some modeling errors in the initial design and despite some amount of parameter drift in the system. The power system environment in some cases may require an extreme degree of robustness in controller design. There have been a few recent papers concerning the design of robust controllers for power system applications.

Chow and Sanchez-Gasca [27] have used frequency response analysis to evaluate PSS controllers at different operating points and to combine them into a single robust controller. In their paper a PSS controller is designed for a one-machine infinite-bus system. The controller is designed to provide machine damping under two operating conditions. One condition has a large line impedance which is referred to as the weak coupling case. The other condition is the same except for with a small line impedance or a strong coupling case. A second-order controller is designed for both of these cases and then they are multiplied by a weighting factor and combined to get a fourth-order controller. Since both controllers have similar frequency responses it is possible to reduce the combined controller to second-order using a

technique called the Hankel Norm algorithm. The frequency response of the resulting controller is approximately the average of the frequency responses of the original two controllers. The authors report that the method does not guarantee stability but is simple to use and provides adequate results when used with good judgement.

A paper by Petrovski and Athans [28] considers the robustness properties of controllers used in a multiterminal DC/AC power system. The authors are interested in using a multiterminal DC system imbedded in an AC power system to enhance overall system damping. A five terminal DC system is used to analyze different control strategies in terms of robustness. The authors are looking at suitable robustness to tolerate actuator and sensor failures, unmodeled dynamics, and changes in system parameters. The authors evaluate robustness by use of two approaches. One way is to introduce errors into the system input transducers and then evaluate the system stability by Lyapunov methods. The size of the error that can be tolerated before instability results is one measure of robustness. In another test the linearized representation of the system is perturbed by a scalar multiplicative factor and also by an additive perturbation matrix, and again stability is assessed by Lyapunov methods. The matrix norm of the perturbation that can be tolerated before instability results is a measure of the robustness of the system. Three decentralized controller designs all involving linear quadratic optimal control strategies are evaluated using these methods, and their relative strengths and weaknesses are tabulated.

Scope and Organization of Remaining Chapters

The following pages are organized into four main parts or chapters. The first part (Chapter 2) contains a detailed description of the program used to carry out the computer simulation of power system dynamics. The second part (Chapter 3) describes the process of controller design using eigenvalue analysis of the linearized system and presents simulation results. The third part (Chapter 4) describes the adaptive controller design and simulation results. The fourth part (Chapter 5) is the conclusion and discussion of aspects warranting further study. The contribution of this work to engineering literature lies primarily in the areas of adaptive control, robust control, and damping control of electrical power systems.

CHAPTER 2

SIMULATION OF POWER SYSTEM DYNAMICS

Introduction

The purpose of this chapter is to describe the methods used for computer simulation of electromechanical oscillations or swing transients of power systems. The major goal of the computer program is to provide a flexible means for simulation of power system dynamics with the same level of detail of modeling that is generally used in the power industry. Computational efficiency, while desirable, is a secondary consideration to program clarity and flexibility in the implementation of control strategies. Modifying an existing code to implement these ideas would seem to be the most efficient course of action. Most commercially available programs however are prohibitively expensive in addition to being cumbersome because of the extensive options that are included. Bonneville Power has a very good swing program that is readily available to the public but its size and lack of documentation make it very difficult to modify. Under these circumstances it was decided to write a program around an available Runge-Kutta integration package called INTEG [29], even though it is generally recognized that trapezoidal integration is more computationally efficient for this type of problem [30],[31].

In general nearly all variables of a power system require some time to respond to a change in the system so that a detailed model of

even a small power system would contain an enormous number of differential equations. The main problem of simulating such a detailed model is the very large range of time constants present or the so-called "stiffness" of the system. To make the simulation practical to implement it is usually necessary to select a time frame of the network behavior which is of interest to study and then make simplifying assumptions for variables which change very rapidly or very slowly compared to this time period. Very small time constants can be changed to zero which transforms the associated differential equation into an algebraic equation. Longer time constants can be made to approach infinity which then turns the variable being simulated into a constant. Time constants associated with the network are very small compared to the electromechanical periods of oscillations, and so it is the usual practice [30],[31] and [32], to assume that network variable changes occur instantaneously. Thus the network variables are treated as algebraic constraints coupled to the differential equations without any significant loss of accuracy. The result of these assumptions is the "quasi-steady-state" network solution utilized in swing programs. Since the system frequency deviation from 60 hertz is very small the network reactances can all be expressed at this frequency with insignificant loss of accuracy. This enables the network variables to be represented as phasor quantities with an implied frequency of 60 hertz. This phasor or steady-state solution of the network variables is updated after changes in the machine state variables are calculated from the integration procedure.

The problem is now formulated as a differential-algebraic initial value problem. The differential equations are solved by Runge-Kutta

integration, and the algebraic constraints on the system are resolved by an iterative procedure at each step of the Runge-Kutta integration. The machine rotor angles relative to the network phasor reference frame are allowed to vary according to differential equations which describe machine rotor speed deviations from the 60 hertz synchronous speed. The resulting network phasor voltages are assumed to always be in steady-state equilibrium with the voltages produced by the machines. Once machine rotor angles and internal voltage magnitudes are determined from the differential equations, the machine and network algebraic relations are solved to determine the voltages and power flows in the network. These network variables then become the forcing functions for the next step in the solution of the differential equations.

Differential Equations

In describing the differential equations used in this swing program the notations and reference frame conventions of [31] are adopted. A more thorough description of machine modeling is given in [33], but the reference frame convention adopted there is different from that in [31]. As mentioned previously this program is written around a Runge-Kutta integration package called INTEG. The INTEG program calls two subroutines, one called SIDE and the other called STATE. The STATE subroutine contains the first-order differential equations or state equations which are integrated by the Runge-Kutta algorithm. The SIDE subroutine contains algebraic constraints on the

differential equations or in our case the machine and network algebraic equations. Both the STATE and SIDE subroutines are contained in a file called 2MIED.FOR which is listed in Appendix A at the end of the thesis.

The majority of the differential equations used in a swing program are of three types: machine mechanical equations; machine electrical equations; and exciter equations. Machine mechanical differential equations describe the motion of the machine rotor angle, relative to its 60 hertz synchronous speed, due to imbalances between mechanical power input to the machine and electrical power output. The rotor angle of each machine in the network is assigned a value based on reference frame conventions which are described in more detail in section 2.3. If δ represents the rotor angle of a machine, then the expression for machine rotor acceleration is

$$d^2\delta/dt^2 = (1/M_g)(P_m - P_e - D(d\delta/dt)) \qquad (2.1)$$

where P_m is mechanical input power, P_e is electrical output power, and M_g is the angular momentum. The constant D is a damping term which is often used to account for damping contributions in the system which are not accurately modeled by other means such as amortisseur windings and nonlinear loads. Rewriting this equation as two first-order differential equations or state equations and neglecting the damping term gives

$$d\omega/dt = (1/M_g)(P_m - P_e) \qquad (2.2)$$

$$d\delta/dt = \omega - 2\pi f_o \qquad (2.3)$$

where f_o is the system base frequency (60 hertz in our case) and ω is

the rotor frequency in radians per second. Another form [32] of this equation utilizes ω as a per-unit quantity in which case the right-hand side of equation (2.3) is replaced by the product of ω and $2\pi f_o$. In this case the steady-state value of ω is zero. Both forms of this equation are widely used and they give the same result in simulations except for a difference in the units being used to represent machine rotor speed. The form shown in (2.3) is used in this work. The electrical power being produced by the machine is a function of voltages and admittances throughout the network to which the machine is connected.

The machine electrical differential equations describe how changes in the machine stator or field currents cause the internal machine voltages to vary. The voltage variations are also influenced by how the machine rotor angle is affecting the path of magnetic fields between the rotor and stator. These differential equations are based on Park's transformation [32], [33]. This mathematical treatment of machine modeling transforms machine impedance values from time-varying, three-phase quantities which depend on machine rotor angle, to constant value parameters in equivalent circuits which lie directly in line with the rotor main axis (the d-axis) or in quadrature with it (the q-axis). This d-q reference frame is fixed to the rotor and moves with the rotor relative to network variables. Different numbers of d and q-axis circuits represent different levels of detailed modeling from slower to very fast time constants. Reference [34] gives a detailed diagram illustrating the interaction between different modeling levels and the machine torques that are developed. The level of modeling used in this program will incorporate slow transient voltages inside the machine as

is usually deemed adequate for this type of study [31]. The differential equations are

$$dE'_q/dt = (E_f - E_q)/T'_{do} = (E_f + (X_d - X'_d)I_d - E'_q)/T'_{do} \qquad (2.4)$$

$$dE'_d/dt = E_d/T'_{qo} = (- (X_q - X'_q)I_q - E'_d)/T'_{qo} \qquad (2.5)$$

and the associated algebraic equations are

$$E'_q - V_q = R_a I_q - X'_d I_d \qquad (2.6)$$

and

$$E'_d - V_d = R_a I_d + X'_q I_q \qquad (2.7)$$

In these equations the subscripts d and q represent direct and quadrature axis quantities respectively. The constant R_a is the armature resistance, E_f is the field voltage, and the time constants T'_{do} and T'_{qo} are transient open-circuit time constants. An explanation of these equations based on heuristic arguments of machine behavior will be given [33].

The machine reactances are the most important parameters for modeling machine behavior, and resistances are often neglected. To determine reactances consider the rotor circuits as closed loop circuits which are not excited. Also the rotor is being turned at synchronous speed, and current of the proper sequence is applied to the armature windings. The voltages measured at the armature terminals can then be used to determine the reactance which is just the measured voltage divided by the applied current. The different reactance values in the equations above are obtained using different rotor positions and either a steady-state current or a suddenly applied current.

Positive sequence, steady-state currents flowing in the armature windings produce a rotating magnetic field inside the machine. If the

main axis or direct axis of the rotor is in line with this rotating flux wave then the flux wave will have its maximum value for a given amount of armature current, and the armature inductive reactance will be at its maximum. This reactance is the direct-axis synchronous reactance. The flux linkage of each armature winding varies sinusoidally with time, and the armature phase voltage induced by the change in this flux wave as it sweeps by the winding is in quadrature with the applied current. The ratio of this voltage to the current is the direct-axis synchronous reactance, X_d.

Now if the rotor is made to rotate at synchronous speed with its interpolar axis or q-axis in line with the rotating flux wave, then the rotating flux wave will have a minimum value. In this case the ratio of the armature voltage component in quadrature with the current, divided by the armature current is the quadrature-axis synchronous reactance X_q.

The conditions under which the transient reactances are defined are the same except that a transient armature current is used rather than a steady-state current. In this case the armature currents are suddenly applied and the voltages are measured immediately after the application of the currents. In the case of the direct-axis transient reactance, X_d', the rotor is rotated with its d-axis in line with the crest of the flux wave. The voltage measured immediately after the application of the armature current is $E_q' = X_d' I_d$ and this eventually decays down to the steady-state value $E_q = X_d I_d$. The time constant associated with this decay is the direct-axis open-circuit time constant T_{do}'. In an analogous way the quadrature-axis open-circuit time constant and transient reactance are defined. In this case

however, the q-axis of the rotor is in line with the armature flux wave. The measured voltage is $E'_q = X'_q I_q$ which in the steady state becomes $E_q = X_q I_q$.

When the field winding is excited, the voltage $E'_d + jE'_q$ is the voltage behind the transient reactance of the machine. The difference between E'_q and E_q is

$$E'_q - E_q = (X'_d - X_d)I_d \tag{2.8}$$

and similarly the difference between E'_d and E_d is

$$E'_d - E_d = (X'_q - X_q)I_q \tag{2.9}$$

In the steady state E_d is zero because the rotor d-axis will be in line with the armature flux wave and no voltage component in phase with the armature current is induced. E'_d however, is not zero but is equal to $(X'_q - X_q)I_q$ provided that X'_q is not equal to X_q (they are usually equal in salient pole machines).

If a sudden change in armature currents occurs then E'_d and E'_q undergo slow changes according to the differential equations (2.4) and (2.5). The values of E_q and E_d however, undergo immediate changes according to the relations

$$\Delta E_q = (X_d - X'_d)\Delta I_d \tag{2.10}$$

$$\Delta E_d = (X_q - X'_q)\Delta I_q \tag{2.11}$$

which can be seen in the right-hand sides of equations (2.4) and (2.5) respectively. Thus the transient voltages will change according to their time constants until they reach steady state where E_q is equal to the field voltage E_f and E_d is zero.

With the field circuit excited the voltage appearing at the generator terminals differs from the internal transient voltages by the voltage drop across the transient reactance and machine armature resistance. This relationship is expressed in equations (2.6) and (2.7) where V_d and V_q are the d and q-axis terminal voltages.

Each machine simulated in this program contains two state equations describing machine mechanical changes, two state equations describing machine internal voltage changes, and three state equations describing the excitation system dynamics. The main purpose of the excitation system is to maintain a constant terminal voltage at the machine bus as system load conditions change by adjusting the field voltage E_f. A standard diagram representation of the excitation system model used is shown in Figure 2. This is an IEEE type I excitation system [35].
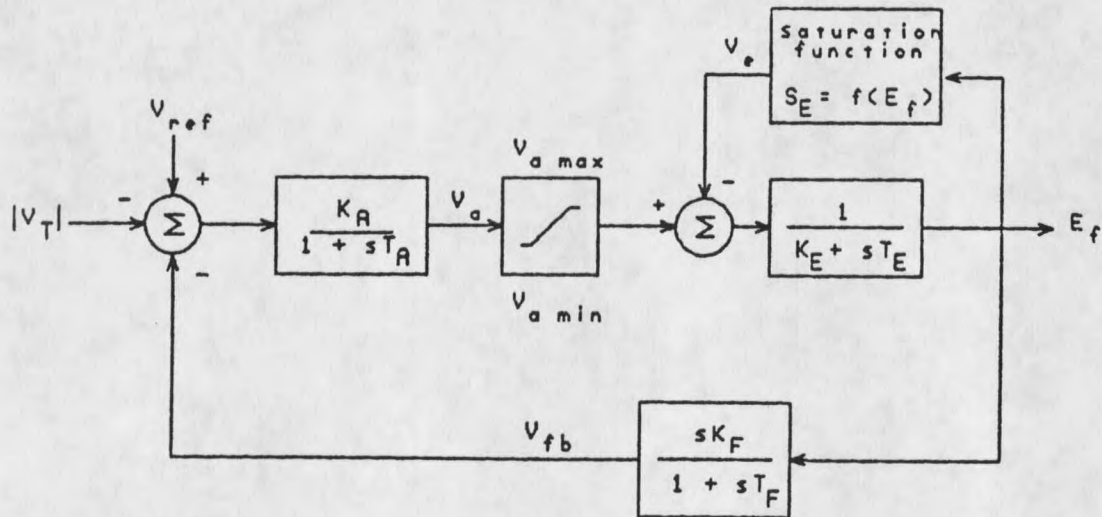
Figure 2.   IEEE type 1 exciter model.

For the forward amplifier in Figure 2, the state equation is

$$dv_a/dt = ((v_{ref} - |v_t| - v_{fb})K_A - v_a)/T_A \qquad (2.11)$$

and for the next linear block it is

$$dE_f/dt = (v_a - v_e - K_E E_f)/T_E \qquad (2.12)$$

while for the feedback block it is

$$dv_{fb}/dt = (K_F(dE_f/dt) - v_{fb})/T_F \qquad (2.13)$$

The above three equations are the differential equations used in each machine to represent changes in the field voltage which then affect the machine internal voltage via equation (2.4) and ultimately the machine terminal voltage magnitude and angle.

The saturation function of Figure 2 is represented as suggested in [31].

$$v_e = (k_1 E_f - k_2)E_f \qquad (2.14)$$

where
$$k_1 = (4S_{0.75max})/(3E_{fmax})$$
$$k_2 = 0.0$$
$$\Big\} \quad \text{if } E_f \leq .75E_{fmax}$$

or

$$k_1 = 4(S_{emax} - S_{e.75max})/E_{fmax}$$
$$k_2 = 4S_{e.75max} - 3S_{emax}$$
$$\Big\} \quad \text{otherwise}$$

where S_{emax} and $S_{e.75max}$ are constants which describe the nonlinearity due to saturation for a particular exciter.

Algebraic Constraints

As mentioned above the algebraic constraints of the system consist mainly of the network equations but also include the machine algebraic relations of equations (2.6) and (2.7). The network behavior is described by the matrix equation

$$I = YV \qquad\qquad (2.15)$$

where I is a vector of complex current injections, Y is the complex nodal admittance matrix and V is the vector of phasor node voltages. The problem here is to solve this equation for the vector V given the current injections of the generators. The solution of these equations involves an iterative procedure because the current injections depend on the machine internal voltages as well as the node voltages that are being solved for. The solution procedure in this program consists of alternately solving for the node voltages and current injections until the values converge to within some error tolerance. For the small time steps necessitated by the stiffness of the system the algebraic relations will usually converge in less than 10 iterations and sometimes may only take 2 or 3 iterations.

The differential and algebraic equations of the machine are written using the d-q reference frame which needs to be reconciled with the real and imaginary reference frame of the network. The d-q reference frame moves with the rotor deviation from its synchronous speed. The real and imaginary reference frame is fixed by choosing a slack bus or reference bus in the network where the voltage angle is

taken to be zero. All other buses in the network have voltage angles relative to this bus. The diagram in Figure 3 illustrates the relation between the two reference frames. The rotor angle δ is taken to be the angle between the real axis of the network and the q-axis of the machine. The convention used here is the same as that used in references [30], [31] and [32] with the d-axis leading 90 degrees in front of the q-axis. There is not a lot of agreement among authors regarding this convention (see [33] or [37]).
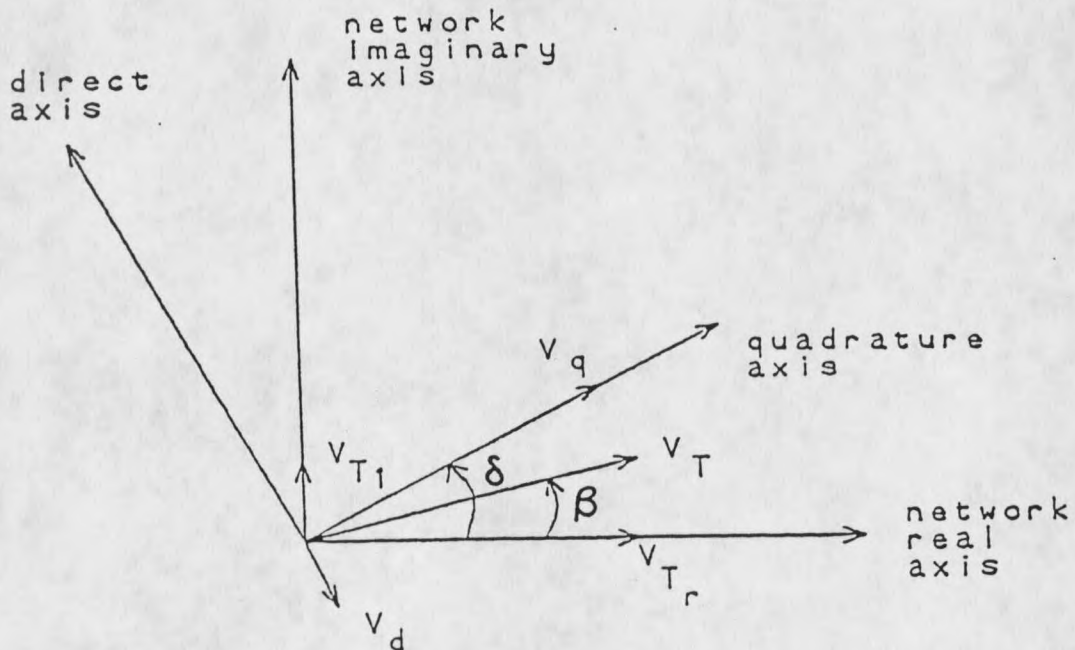
Figure 3. Phasor diagram of reference frames.

In order to relate the machine internal voltages to the network voltages it is necessary to transform the variables back and forth between the d-q axes and the real and imaginary network axes. Analysis of the relations illustrated in Figure 3 shows the transformation to be

$$
\begin{bmatrix} V_r \\ V_i \end{bmatrix} = \begin{bmatrix} \cos(\delta) & -\sin(\delta) \\ \sin(\delta) & \cos(\delta) \end{bmatrix} \begin{bmatrix} V_q \\ V_d \end{bmatrix} \tag{2.16}
$$

or in the reverse direction

$$
\begin{bmatrix} V_q \\ V_d \end{bmatrix} = \begin{bmatrix} \cos(\delta) & \sin(\delta) \\ -\sin(\delta) & \cos(\delta) \end{bmatrix} \begin{bmatrix} V_r \\ V_i \end{bmatrix} \tag{2.17}
$$

The δ used here is the same δ used as the rotor angle in the electromechanical equations (2.3). Also the transformations used here are the same if currents are substituted for voltages.

The solution of the algebraic constraints starts once the machine rotor angles, δ's, have been computed from the differential equations along with the machine internal transient voltages E'_d and E'_q. The first step of the solution procedure then is to solve for the machine internal d and q axis currents as a function of the above variables and then find the injection currents so that the network admittance matrix equations can be solved. Axis transformations from the machine reference frame to network and back are performed at the appropriate places. The entire process is iterated until the machine voltages and currents converge. The sequence of the equations is shown below. In these equations only one machine is represented. In a multimachine system each set of equations is repeated once for each machine.

$$
V_q = V_{T_{real}} \cos(\delta) + V_{T_{imag}} \sin(\delta) \tag{2.18a}
$$

$$
V_d = -V_{T_{real}} \sin(\delta) + V_{T_{imag}} \cos(\delta) \tag{2.18b}
$$

$$
\vdots
$$

$$I_d = \frac{R_a(E'_d - V_d) - X'_q(E'_q - V_q)}{(R_a^2 + X'_q X'_d)} \qquad (2.18c)$$

$$I_q = \frac{R_a(E'_q - V_q) + X'_d(E'_d - V_d)}{(R_a^2 + X'_q X'_d)} \qquad (2.18d)$$

$$\vdots$$

$$I_{T_{real}} = I_q \cos(\delta) - I_d \sin(\delta) \qquad (2.18e)$$

$$I_{T_{imag}} = I_q \sin(\delta) + I_d \cos(\delta) \qquad (2.18f)$$

$$\vdots$$

$$I_T = I_{T_{real}} + j I_{T_{imag}} \qquad (2.18g)$$

$$V_T = V_{T_{real}} + j V_{T_{imag}} \qquad (2.18h)$$

$$\vdots$$

solve for the vector V

$$I = YV \qquad (2.18i)$$

This loop is iterated until the values being calculated on the left-hand side of these equations have converged to within some error tolerance. Once this occurs then the electrical power out of the machine is calculated from

$$P_e = V_d I_d + V_q I_q \qquad (2.19)$$

This value of machine electrical power then goes into determining the machine accelerating power in the differential equation (2.2).

Equation (2.15) (which is the same equation as (2.18i)) is not actually solved in matrix form; instead the equations are written out

individually in terms of nonzero elements of the admittance matrix and then rearranged to obtain the bus voltages. As an example the nine-bus system used here has the generator current injection at bus #1 expressed as

$$I_{T_1} = Y_{11}V_{T_1} + Y_{14}V_{T_4} \qquad (2.20)$$

which is then rearranged to

$$V_{T_1} = (I_{T_1} - Y_{14}V_{T_4})/Y_{11} \qquad (2.21)$$

Taking bus #4 as an example of a non generator bus, the admittance matrix equation has the form

$$0 = Y_{41}V_{T_1} + Y_{44}V_{T_4} + Y_{45}V_{T_5} + Y_{46}V_{T_6} \qquad (2.22)$$

which is rearranged to

$$V_{T_4} = -(Y_{41}V_{T_1} + Y_{45}V_{T_5} + Y_{46}V_{T_6})/Y_{44} \qquad (2.23)$$

There are two techniques which have been implemented into the program to help speed up the convergence rate of the solution of the algebraic equations. One technique is to iterate the nongenerator network equations as represented by (2.23) within the larger loop. In this program the nongenerator bus voltages are iterated k times where k is equal to the number of nongenerator buses. This significantly improves the convergence rate of the overall loop. In many industrial programs the admittance matrix is reduced by partitioning the Y matrix and substituting variables so that equation (2.18i) has only generator buses being represented in the V vector. This has been reported to help increase the rate of convergence [30]. The procedure used here of

iterating the nongenerator buses has the same effect but avoids having to recompute the reduced Y matrix whenever the SVC susceptance value is changed. Although this procedure forms an inner loop within the overall iterative solution scheme, it has been found that the total amount of computing needed is significantly reduced. The choice of iterating these equations k times is based on trial and error analysis; it is possible that even fewer iterations would give satisfactory results.

The other method used to improve convergence entails extrapolating the angle change of the generator bus voltages before the solution of the algebraic equations is started as suggested in [36]. In this procedure the change in the machine rotor angle from the value at the previous time step is used to estimate the bus voltage angle solution before the iterative solution is begun. This procedure has been found to decrease the total number of iterations needed before convergence but not as significantly as the previously described procedure.

There are two different criteria used to determine when convergence is reached. If the variable has an absolute value less than 0.0001, the criterion for convergence is to have an absolute change from the previous iteration of less than 0.0001. If the variable has an absolute value greater than 0.0001 then a relative change of less than 0.0001 (or a change of less than 0.01%) from the previous iteration is used as the criterion. The entire loop is iterated until all the variables have passed one or the other of these convergence criteria.

Besides the equations contained in the main loop (2.18a-i) of the SIDE subroutine described above, there are other calculations performed

which include saturation functions for the excitation systems and timing functions for use in calling the identification and control subroutines which will be discussed in later chapters. There is also some logic implemented to simulate disturbances in the system network.

There are two types of disturbances which can be simulated in this program. One type is the usual short circuit or switching fault commonly represented in swing programs by changing one or more elements in the network admittance matrix. There is usually some logic associated with changing the entries of the admittance matrix to correspond to the time period when the short circuit is applied, the time when the transmission line is opened, and the time when the line is reclosed.

The second type of disturbance that can be simulated is often referred to as an exogenous disturbance input or noncontrollable input disturbance. This type of disturbance is used to test the effectiveness of control strategies in damping oscillations which cannot be completely eliminated from the system. The disturbance can be simulated by modulation of the infinite-bus voltage magnitude. In this program, a sinusoid of some selected frequency (e.g. 0.3 hertz) with a magnitude of around 10 per cent of the normal voltage magnitude can be·added to the infinite-bus voltage.

Initial Conditions

Before a simulation of power system electromechanical oscillations can begin it is necessary to establish the system initial conditions

and to specify the type of disturbance to be introduced into the system [30], [32]. A load-flow solution of the network is used to establish the steady-state operating point of the network from which the swing transients begin when a disturbance is introduced. In addition to obtaining the network steady-state operating point, it is necessary to calculate the machine steady-state conditions also. This can be done with the help of the phasor diagram shown in Figure 4. In this diagram δ is the machine rotor angle, β is the angle of the generator bus voltage, and ϕ is the angle by which the bus current lags the bus voltage or the power factor angle.
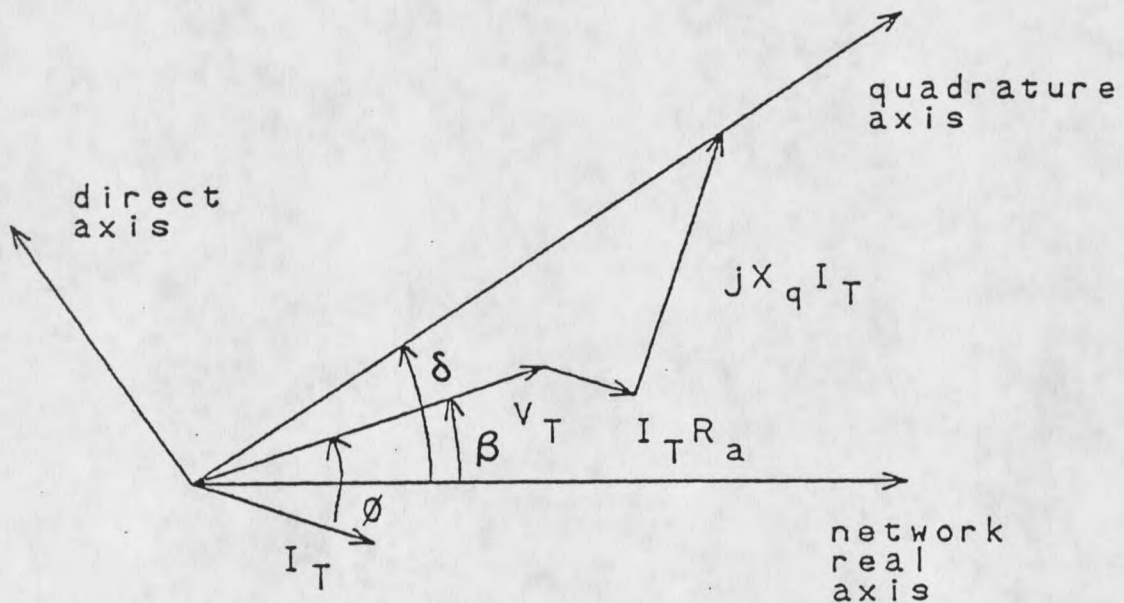
Figure 4. Phasor diagram of machine steady-state conditions.

The load flow solution gives the generator terminal bus voltage (V_T) and the real and reactive power (P,Q) being supplied by each

generator. Given this information it is necessary to solve for the steady-state values of E_q', E_d', E_f and δ for each machine. First the steady-state current injected into each bus is found from the relation

$$I_T = (P - jQ)/V_T^* = I_{T_{real}} + jI_{T_{imag}} \tag{2.24}$$

where P and Q are the real and reactive power injections and V_T^* is the conjugate of the generator bus terminal voltage. The rotor angle δ can be found using Figure 4, which illustrates the relation

$$\tan(\delta) = \frac{V_{T_{imag}} + X_q I_{T_{real}} + R_a I_{T_{imag}}}{V_{T_{real}} + R_a I_{T_{real}} - X_q I_{T_{imag}}} \tag{2.25}$$

This equation results from the fact that at steady state, the voltage drop of the terminal current flowing through the armature resistance and the q-axis reactance, when added to the terminal voltage, produces a voltage vector which lies on the machine q-axis. This relationship is not obvious and to explain why it is true, consider the steady-state equation

$$E_q = V_T + R_a I_T + jX_q I_q + jX_d I_d \tag{2.26}$$

This equation is true since E_d is zero at steady state so the internal machine voltage must lie entirely along the q-axis. If X_d in (2.26) is replaced with X_q then the result is a vector, $\hat{E}_q$, which is colinear with E_q but has a different magnitude.

$$\hat{E}_q = V_T + R_a I_T + jX_q I_T \tag{2.27}$$

This equation is the relation which gives equation (2.25). Verification that this vector falls on the q-axis is based on the fact that both jX_qI_d and jX_dI_d are vectors which are parallel to the q-axis, but differ in length. Substituting jX_qI_d for jX_dI_d in (2.26) results in (2.27) and produces a vector which lies on the q-axis, but has a different length than Eq, and no physical interpretation other than being a usefull construct. The objective here is to find the angle δ. Equation (2.26) cannot be used because I_d and I_q cannot be found without first knowing δ. It is possible however to use (2.27) to locate the q-axis, given only the real and imaginary components of machine terminal voltage and current, then find the angle δ via (2.25). Once δ is determined then the d and q-axis components of the terminal voltage and current can be found. Verification of (2.25) can be found in [30], [32] or [33].

The machine terminal variables can now be projected onto the d and q axes by the relations

$$V_d = -|V_T|\sin(\delta - \beta) \tag{2.28}$$

$$V_q = |V_T|\cos(\delta - \beta) \tag{2.29}$$

$$I_d = -|I_T|\sin(\delta - \beta + \phi) \tag{2.30}$$

$$I_q = |I_T|\cos(\delta - \beta + \phi) \tag{2.31}$$

The value of E_d' is then found by setting the differential equation

of (2.5) to zero to obtain

$$E'_d = (X'_q - X_q)I_q \qquad (2.32)$$

The steady-state value of E'_q is found from the algebraic relations of equation (2.6) to give

$$E'_q = -X'_d I_d + R_a I_q + V_q \qquad (2.33)$$

Finally the steady-state value of the field voltage E_f is found by setting the differential equation (2.4) to zero to obtain

$$E_f = E'_q - (X_d - X'_d)I_d \qquad (2.34)$$

The steady-state electrical power out of the machine is the same as that calculated by equation (2.19).

These calculations are performed by a program called ICFIND.FOR which is listed in Appendix B at the end of the thesis. The initial conditions calculated by this program are printed out to a file in a format which can be read by the INTEG program at the beginning of its execution. Also supplied by the program are other initial conditions which are zero or need no calculation, such as the steady-state rotor angular velocity (376.99 radians/sec).

CHAPTER 3

FIXED COMPENSATOR DESIGN PROCEDURE

Introduction

This chapter presents an approach to developing control strategies for SVC control to enhance system damping. The approach taken is to develop a nonadaptive or fixed control strategy based on a computer generated linearization of the nonlinear power system model. Eigenvalue analysis of the linearized system is used to design a feedback compensator. An effort is made to incorporate robustness in controller design so that system damping can be improved at more than one system operating point.

The controller design is developed and evaluated on a nine-bus power system which is based on data presented in [32]. A one-line diagram of the system is illustrated in Figure 5, and the machine and network data are listed in Table 1. This power system is essentially the same as that listed in the reference with the addition of exciter models at machines #2 and #3 and the addition of the SVC at bus 8. Also generator #1 is being modeled as an infinite bus in order to provide a stationary reference for the evaluation of rotor oscillations of the other two machines. The SVC is modeled as a variable shunt susceptance which is added to the system admittance matrix before the solution of the network equations.

Table 1. Machine and network data

Exciter and AVR Data		
Parameters	Gen #2	Gen #3
K_A	25.0	25.0
T_A	0.20	0.20
K_F	0.091	0.105
T_F	0.35	0.35
K_E	−0.0505	−0.0582
T_E	0.5685	0.6544
E_{Fmax}	3.96	3.438
S_{Emax}	0.303	0.349
$S_{E.75max}$	0.0778	0.0895

Machine Data (100 MVA base)			
Parameters	Gen #2	Gen #3	Gen #1
x_d	0.8958	1.3125	(Inf bus)
x'_d	0.1198	0.1813	
x_q	0.8645	1.2578	0.0969
x'_q	0.1969	0.25	
T'_{d0}	6.00	5.89	
T'_{q0}	0.535	0.60	
H	6.40	3.01	

Transmission Line and Transformer Data			
bus #	R	X	B/2
4–5	0.010	0.085	0.088
5–7	0.032	0.161	0.153
7–8	0.0085	0.072	0.0745
8–9	0.0119	0.1008	0.1045
9–6	0.039	0.170	0.179
6–4	0.017	0.092	0.079
1–4		0.0576	
2–7		0.0625	
3–9		0.0586	

Steady-State Conditions				
bus #	P(gen)	Q(gen)	$|V|$	delta(°)
1	0.716	0.27	1.04	0.0
2	1.63	0.067	1.025	9.3
3	0.85	−0.109	1.025	4.7
4	0.0	0.0	1.026	−2.2
5	−1.25	−0.50	0.996	−4.0
6	−0.90	−0.30	1.013	−3.7
7	0.0	0.0	1.026	3.7
8	−1.00	−0.35	1.016	0.7
9	0.0	0.0	1.032	2.0
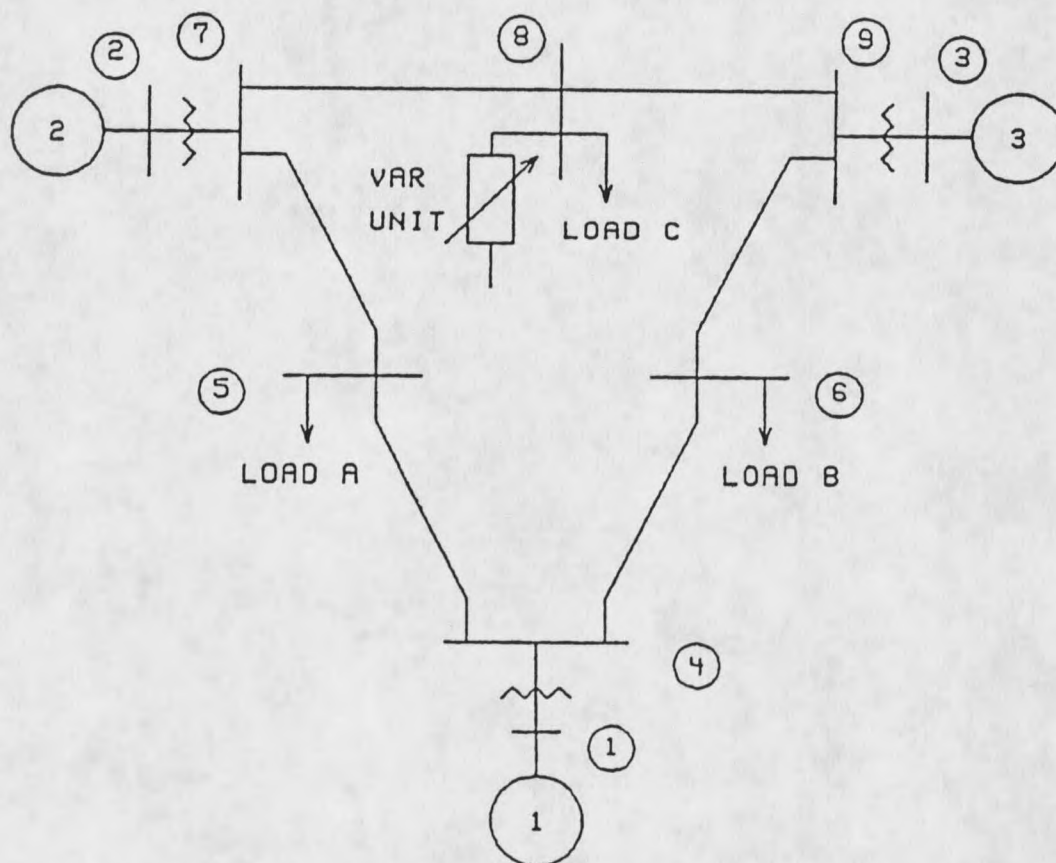
Figure 5. One-line diagram of the nine-bus network.

The methods for simulating the power system were explained in the previous chapter. This system uses seven differential equations for each generator, #2 and #3, plus two more differential equations to represent the feedback compensator for a total of 16 differential equations. A useful feature of this particular simulation method is the ease with which it lends itself to a computer generated system linearization.

A control strategy for an SVC can be developed based on an intuitive approach for a one-machine infinite-bus system. When the

machine rotor angle velocity is positive, then the machine is building up kinetic energy which can be reduced by increasing the line voltage, thus increasing the electrical power out of the machine. Similarly, when the machine rotor angle velocity is negative, the size of the oscillation can be reduced by lowering the line voltage and decreasing the electrical power out of the machine. Thus to dampen machine oscillations the var unit susceptance presented to the system can be calculated by multiplying the state variable representing machine velocity times some suitable gain. In a multimachine case the var unit can be controlled by using the local bus frequency deviation rather than the rotor velocity of a particular machine. While this type of strategy may work well under certain circumstances, it often happens that damping will be increased in the main critical modes but decreased in other critical modes. Another consideration in practical applications is that there will be some time delay and phase shift associated with the instrumentation that measures the local bus frequency deviation. Thus it is very likely that a compensator will be needed in the feedback loop in order to obtain improved system damping although some damping may be obtainable without such a compensator.

Some of the papers reviewed in Chapter 1 report on results using various system signals for feedback without a compensator with some success. The problem of designing control compensators for power systems is difficult because of the nonlinear and time varying nature of such systems. Most design procedures for controllers are based on linear system models, so that to use these techniques it is necessary to linearize the power system model.

The Linearization Procedure

The previous chapter discusses in detail how the power system is modeled as a set of differential equations with algebraic constraints. The set of nonlinear differential equations representing system dynamics can be expressed as

$$\underline{\dot{x}} = \underline{f}(\underline{x}, \underline{z}) \tag{3.1}$$

where $\underline{x}$ is a vector of state variables and $\underline{z}$ represents the side variables such as network bus voltages and currents, machine accelerating power, machine currents, etc. The vector $\underline{f}$ consists of functions of the state and side variables. The side equations represent algebraic conditions, such as Ohms law for the network variables, that must be satisfied at each integration step and these conditions are expressed as

$$\underline{g}(\underline{x}, \underline{z}) = 0 \tag{3.2}$$

In order to design a nonadaptive feedback compensator for var unit control using well established control concepts, a computerized method was developed to linearize the system into a linear state-space representation of the form

$$\Delta\underline{\dot{x}} = A\Delta\underline{x} \tag{3.3}$$

where A is the Jacobian matrix. This set of equations contains the states of each machine and also accounts for the effects of the var unit, the network interconnections, and the feedback compensator. The

linearization is done by applying small perturbations to each of the states (one at a time) and evaluating the resulting derivatives. The ratio of the derivative to the perturbation size then determines the coefficients of the A matrix. As an example consider the linear state-space representation shown below.

$$
\begin{bmatrix} \dot{x}_1 \\ \dot{x}_2 \\ \vdots \\ \dot{x}_n \end{bmatrix} = \begin{bmatrix} a_{11} & a_{12} & \cdots & a_{1n} \\ a_{21} & a_{22} & \cdots & a_{2n} \\ \vdots & & & \vdots \\ a_{n1} & a_{n2} & \cdots & a_{nn} \end{bmatrix} \begin{bmatrix} x_1 \\ x_2 \\ \vdots \\ x_n \end{bmatrix} \qquad (3.4)
$$

The linearization procedure is performed at a steady-state operating point. At steady state, each of the derivatives is equal to zero. When state variable one is perturbed away from equilibrium, then the state derivatives are calculated from

$$
\dot{x}_{i1} = a_{i1}(x_1 + \Delta x_1) + a_{i2}x_2 + \cdots + a_{in}x_n \qquad (3.5)
$$

or

$$
\dot{x}_{i1} = a_{i1}x_1 + a_{i2}x_2 + \cdots + a_{in}x_n + a_{i1}\Delta x_1 \qquad (3.6)
$$

The second subscript on $\dot{x}_{i1}$ is used to emphasize the fact that this value results from the displacement Δx_1.

Theoretically each state variable in (3.6) is at its equilibrium value, in which case the first n terms of (3.6) will sum to zero. In practice however the equilibrium values may only be known to three or four places; this results in a small but nonzero contribution which we will call the offset, k_i:

$$k_i = a_{i1}x_1 + a_{i2}x_2 + \cdots + a_{in}x_n \qquad (3.7)$$

where all x's are at or very near their equilibrium values. When x_1 is perturbed away from its equilibrium value the coefficients in the first column of the A matrix are found from the relation

$$a_{i1} = (\dot{x}_{i1} - k_i)/\Delta x_1 \qquad (3.8)$$

Similarly the coefficients of the second column are found from

$$a_{i2} = (\dot{x}_{i2} - k_i)/\Delta x_2 \qquad (3.9)$$

and in general the relation is

$$a_{ij} = (\dot{x}_{ij} - k_i)/\Delta x_j \qquad (3.10)$$

To find the linear model coefficients from the nonlinear system model, the nonlinear functions, f_i's, are each evaluated at the approximate equilibrium point to determine the offsets, k_i's. Then one state is perturbed away from equilibrium while all the others remain at their steady-state values. Let $\underline{x}_j$ represent the values of $\underline{x}$ that results when the jth component of $\underline{x}$ is perturbed by the amount Δx_j. Also, let $\underline{z}_j$ be the corresponding value of $\underline{z}$ that satisfies the side equations; that is,

$$\underline{g}(\underline{x}_j, \underline{z}_j) = 0 \qquad (3.11)$$

The vector pair $\underline{x}_j$, $\underline{z}_j$ are used to evaluate the derivatives as follows:

$$\underline{\dot{x}}_{ij} = \underline{f}_i(\underline{x}_j, \underline{z}_j) \qquad (3.12)$$

Once the derivatives are evaluated, the coefficients for the linear
system are calculated as shown in (3.10).

For the system studied here, the value of Δx_j was determined as
follows. A moderate system disturbance was simulated, and the maximum
deviation of the jth variable away from equilibrium was recorded. Ten
percent of the absolute value of this deviation was then used to define
Δx_j. In this power system the coefficients being calculated were not
very sensitive to the size of the perturbations used.

Using this linearization procedure, one can obtain an A matrix for
different feedback settings and compensator designs using the same
subroutines that are used to carry out the time response simulations.
Each different A matrix has a set of eigenvalues which will move as the
parameters of the system are adjusted. Computer codes, such as the
NASA (National Aeronautics and Space Administration) ORACLS program
[38] used here, are widely available for calculating the eigenvalues.
By varying the gain for a particular compensator, a root locus type of
plot of the system eigenvalues can be obtained.

The subroutine EIGEN in the ORACLS package computes all the
eigenvalues of a two-dimensional A matrix. The matrix is passed in the
argument list of the subroutine which balances it and reduces it to
upper Hessenberg form. All of the eigenvalues are then found by the
double shift QR algorithm [38].

In developing this linearized model for controller design
purposes, it is necessary to select a system output signal for feedback
which will be easy to compute in the linearization process. Since time
is not a variable represented in the linearization process, it is not
convenient to use frequency deviation calculated as change in bus angle

divided by change in time. Consequently the simulations presented in this chapter use local bus angle deviation from the steady-state value as the signal that is fed back through the compensator.

Fixed Compensator Design

The fixed compensator design was initiated by linearizing the 9-bus system so that a 16th-order A matrix was obtained. Each machine was represented by seven states and the compensator by two states. The input to the compensator is local bus voltage angle deviation and its output is the value of var unit susceptance to be presented to the network.

A circuit diagram of the compensator used in this program is given in Figure 6. The two state equations describing the behavior of this circuit are

$$dV_2/dt = k_1(V_1 - V_2) \qquad (3.13)$$

$$dV_3/dt = dV_2/dt - V_3k_2 \qquad (3.14)$$

where $k_1 = 1/(R_2C_2)$ and $k_2 = 1/(R_3C_3)$. The overall transfer function of the compensator is

$$\frac{V_3}{V_1} = \frac{k_1s}{(s + k_1)(s + k_2)} \qquad (3.15)$$

As is indicated by (3.15) the compensator structure contains a zero at the origin in the s plane in order to filter out any DC component in

the feedback signal. It also has two poles, which give it a bandpass characteristic, and whose locations are adjustable. In the computer program the output of this filter, V_3, is multiplied by a constant, G, which determines the susceptance value of the SVC that goes into the admittance matrix before the network solution is calculated. This constant serves as a gain which enables the gain of the overall compensator to be adjusted independently of k_1.
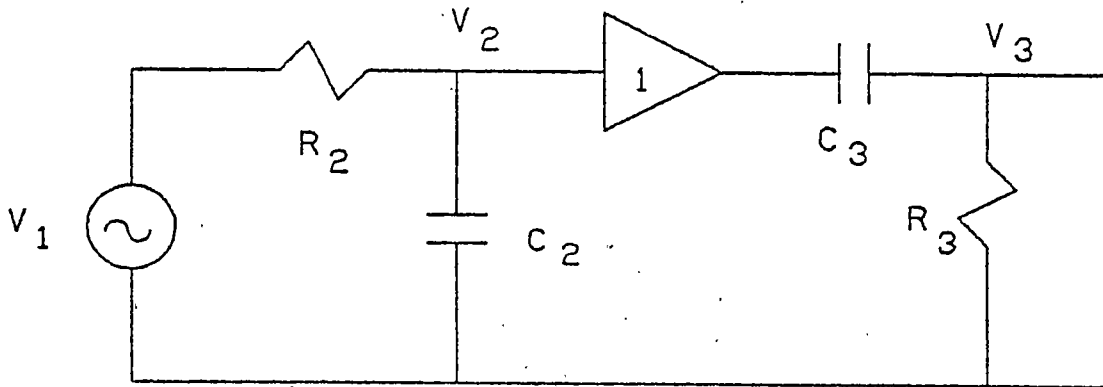
Figure 6. Diagram of compensator circuit.

By iteratively adjusting these three parameters, k_1, k_2, and G, and watching the location of the three or four eigenvalues closest to the $j\omega$ axis, it is possible to find a set of compensator parameters that provide the maximum amount of damping for that particular operating point. In order to incorporate robustness in the controller design it is necessary to map out acceptable parameter regions for different operating points to identify the set of parameter values which provides the maximum amount of damping for each of the operating points being

considered. In this particular case the same controller structure is capable of providing a significant amount of damping for both operating points which are being considered.

The program written to perform this linearization and eigenvalue analysis is called LAD and is listed in Appendix C. This program calls the same subroutines STATE and SIDE used by INTEG and listed in Appendix A. When the program is run it first reads the initial condition information used by INTEG, and this data contains the steady-state values of the state variables. Another file called MAXX.OUT also is read which contains the information to be used for perturbing each of the states. The user is prompted to enter the gain, G, and the corner frequencies of the compensator, k_1 and k_2. With this information the system is linearized with the feedback loop in place and the eigenvalues are calculated. The eigenvalues are then searched and any of them having real parts greater than -0.4 are displayed on the screen. The program again prompts for new values of G, k_1, and k_2, so the user can watch what effect changing each of these values has on the eigenvalues of the system. With G set at zero, the feedback loop is open and there are four eigenvalues that appear on the screen. These are listed in Table 2 along with the eigenvalues that appear on the screen for some other sets of parameters. After some experimentation with the three compensator parameters an approximately optimal set of parameters can be found. The eigenvalues which appear on the screen for this case also are listed in Table 2. The table lists some eigenvalues for two different system operating points. Operating point A is the steady-state condition illustrated by the diagram in Figure 5 and listed in Table 1. Operating point B is the same network except

line 4-5 is disconnected and the resulting system steady-state condition is calculated from a load-flow solution and the ICFIND program.

Simulation Results

Figure 7 illustrates generator rotor angle responses to a three-phase fault on line 5-7 which begins at t=0.1 seconds and lasts for three cycles. The line is then opened for six cycles and reclosed again with the fault removed. In this case (Figure 7) there is no var unit control to dampen oscillations. The system exhibits two lightly damped modes, one at about 1.1 hertz and the other at about 0.15 hertz. This case corresponds to the first entry in Table 2 where four critical sets of eigenvalues are identified.

Figure 8 illustrates the same disturbance but now the var unit is being controlled by feedback through the compensator. For this simulation the compensator has corner frequencies at 5.5 and 0.1 hertz and the output is then multiplied by a gain of 4.0. A significant improvement in system damping is obtained. Table 2 indicates only one critical system mode for this set of parameters and this mode does not involve the machine rotor angles to a great degree. This mode is also not effected very much by any changes in the compensator parameters.

Figure 9 illustrates another disturbance with no var unit control. This disturbance is caused by disconnecting line 4-5 with no reclosing, thus forcing the system to find a new operating point. As the figure indicates the higher frequency mode appears to be unstable. This case

is listed as the last entry in Table 2 which indicates the higher frequency mode is stable but with very slight damping. Two other critical modes are also present.

Table 2. Compensator parameters and resulting critical eigenvalues of the system.

K_1	K_2	G	EIGENVALUES
OPERATING POINT A -- SEE FIG 3.1			
$2\pi 10.0$	$2\pi 0.005$	0.0	$-0.0314 \pm j2\pi 0.00$
			$-0.1319 \pm j2\pi 0.0807$
			$-0.1347 \pm j2\pi 0.1496$
			$-0.1126 \pm j2\pi 1.1088$
$2\pi 5.5$	$2\pi 0.1$	4.0	$-0.1366 \pm j2\pi 0.0809$
$2\pi 5.5$	$2\pi 0.1$	2.0	$-0.1342 \pm j2\pi 0.0807$
			$-0.2548 \pm j2\pi 0.1755$
			$-0.3360 \pm j2\pi 0.9554$
OPERATING POINT B -- LINE 4-5 OPENED			
$2\pi 5.5$	$2\pi 0.1$	4.0	$-0.1469 \pm j2\pi 0.0831$
			$+1.9220 \pm j2\pi 0.2626$
$2\pi 5.5$	$2\pi 0.1$	2.0	$-0.1512 \pm j2\pi 0.0838$
			$-0.3123 \pm j2\pi 0.6678$
$2\pi 5.5$	$2\pi 0.1$	0.0	$-0.1550 \pm j2\pi 0.0844$
			$-0.1801 \pm j2\pi 0.1519$
			$-0.0064 \pm j2\pi 0.9637$

Figure 10 illustrates the machine response to this open-line disturbance with the same var unit control design as used in Figure 8. The illustration shows that the system is unstable but now with different dominant modes. The point to be made here is that a fixed compensator that enhances system damping under one set of conditions may not be appropriate for a different set of system conditions. This case is listed in Table 2 where an unstable eigenvalue is indicated along with another critical mode which is stable. It is evident from the values listed in the Table that the control strategy is very effective under one set of conditions but actually detrimental to system performance under another set of system conditions.

There are undoubtedly other compensator structures and settings that are more robust in terms of providing increased system damping for a variety of system operating points and disturbances. It has been found that a compensator with corner frequencies of 5.5 and 0.1 hertz and a gain of 2.0 will result in a stable system for the open-line disturbance but with some decreased effectiveness for the three-phase fault disturbance. Figures 11 and 12 illustrate the time domain effectiveness of this compensator for the two different disturbances. The two cases are also presented in Table 2 where it is evident that the new settings improve the eigenvalues of the open-line system while the eigenvalues of the original system are not as good but still acceptable. The difficulty in finding the best controller will undoubtedly involve a compromise between effectiveness and robustness as well as determining how much robustness is necessary. An efficient means of approaching the problem especially for a large power system has yet to be developed.
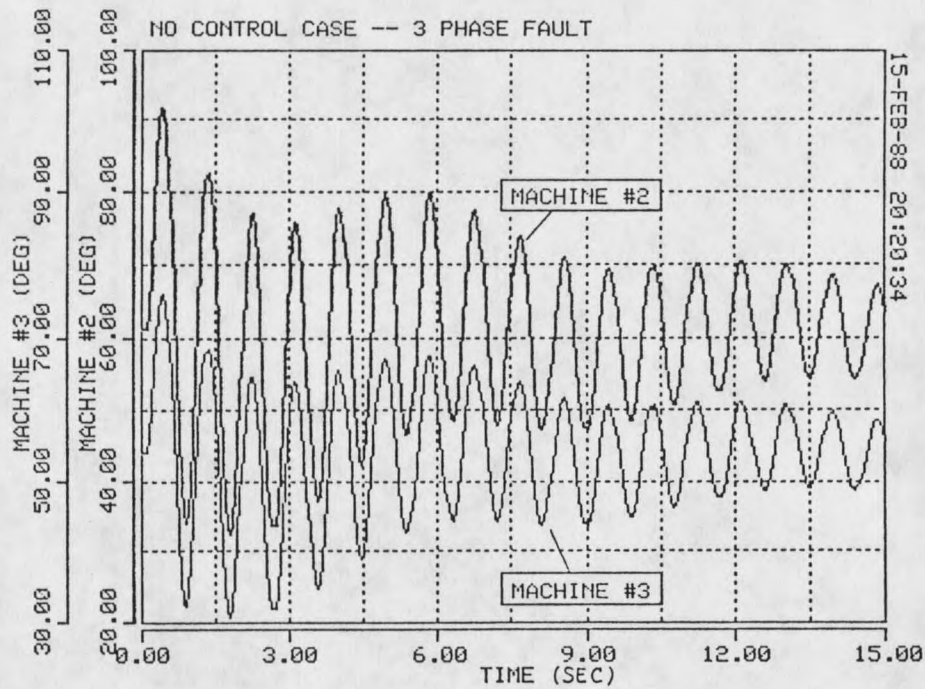
Figure 7.   Three-phase fault disturbance with no var unit control.

Figure 8.   Three-phase fault disturbance with fixed controller
parameters $k_1 = 2\pi 5.5$, $k_2 = 2\pi 0.1$, and $G = 4.0$.
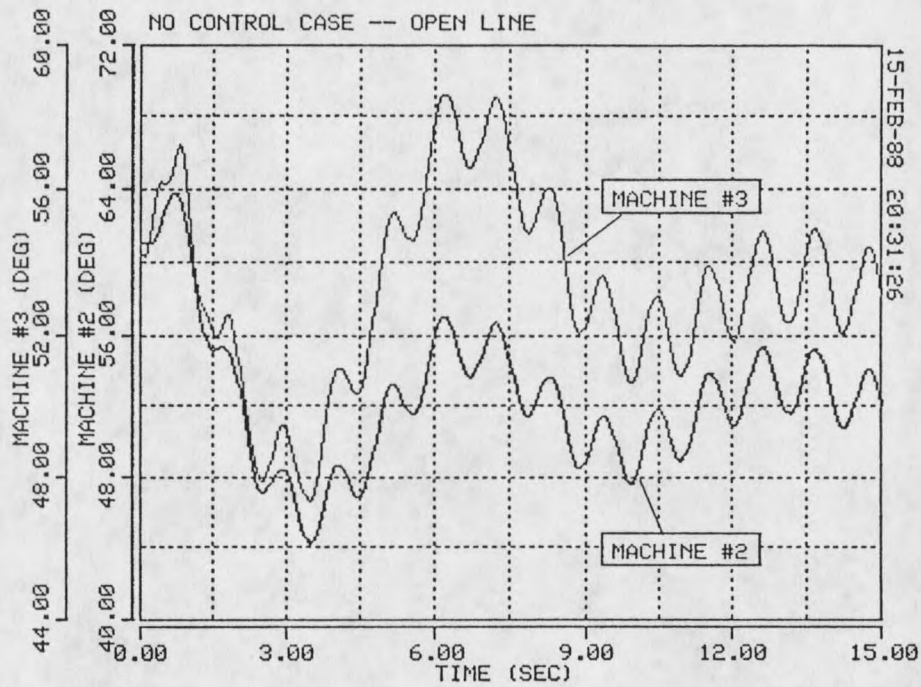
Figure 9.   Open-line disturbance with no var unit control.
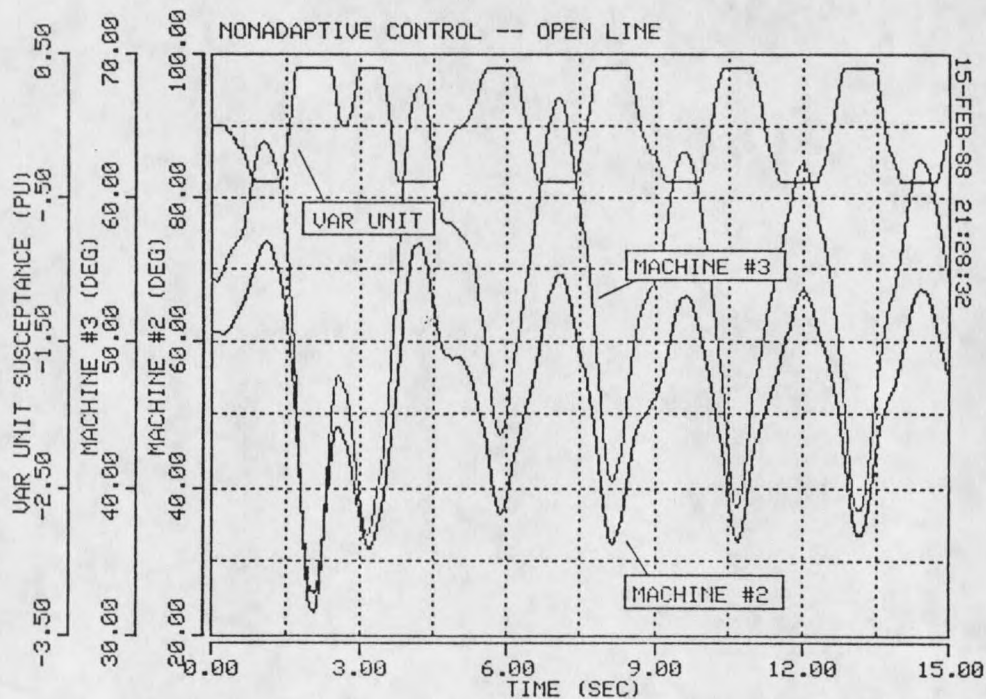
Figure 10.   Open-line disturbance with fixed controller parameters
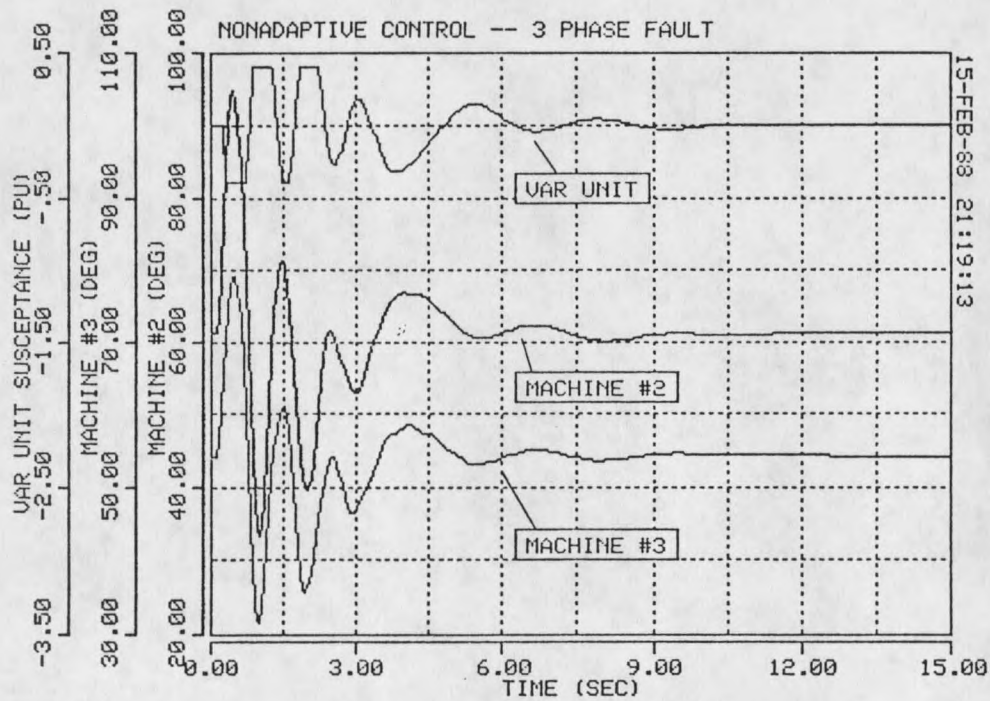$k_1 = 2\pi5.5$, $k_2 = 2\pi0.1$, and G = 4.0.

58
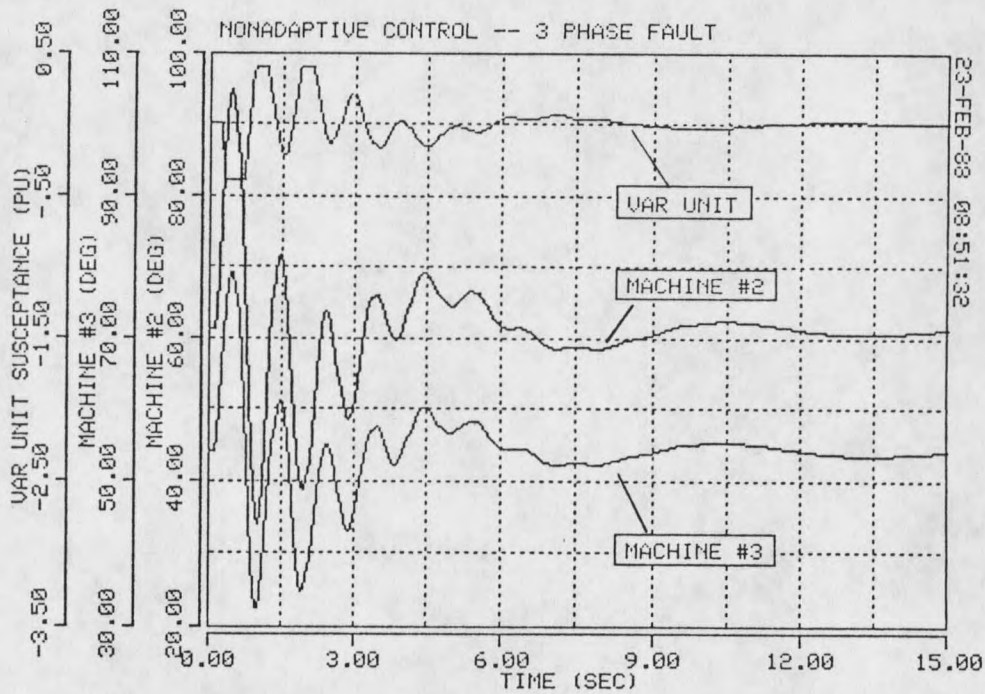
Figure 11. Three-phase fault disturbance with fixed controller
parameters $k_1 = 2\pi5.5$, $k_2 = 2\pi0.1$, and $G = 2.0$.
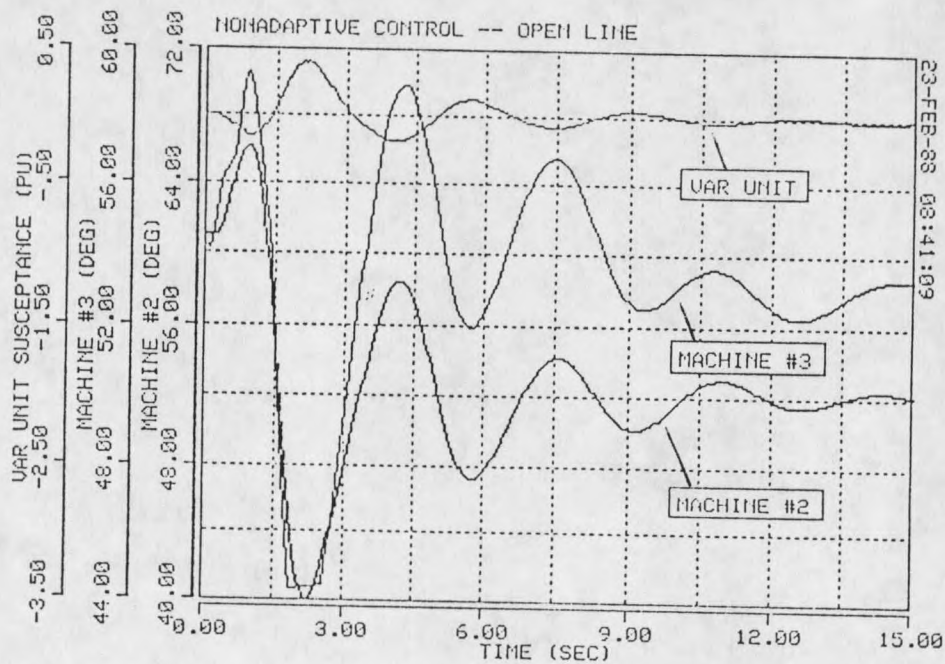
Figure 12. Open-line disturbance with fixed controller parameters
$k_1 = 2\pi5.5$, $k_2 = 2\pi0.1$, and $G = 2.0$.

CHAPTER 4

AN ENHANCED LQ ADAPTIVE CONTROLLER

Introduction

The purpose of this chapter is to describe an adaptive linear–quadratic–Gaussian (LQG) control strategy which is used to control the susceptance that a static var compensator (SVC) presents to a power system network so as to improve the damping of machine oscillations in the system. Computer simulation results are presented to illustrate the effectiveness of the controller in damping machine oscillations which occur due to power system disturbances.

The application of an adaptive LQG controller to control var–unit susceptance in order to enhance overall system damping has several advantages. The controller is tolerant of nonminimum phase systems; it does not require knowledge of the order of the system being controlled; and it can tolerate cases where the identified model of the plant contains common factors in its numerator and denominator polynomials. The algorithm presented here is patterned after those presented in references [39], [40], [41], and [42] with some modifications [23]. The modifications reduce the high–frequency gain of the controller and thereby decrease the possibility of subsynchronous mode excitation.

The overall system to be considered here combines an adaptive controller and the power system (or plant), as shown in Figure 13. The adaptive controller has three components: 1) an on-line identifier, 2)

an adaptive observer, and 3) an adaptive LQG controller. Control is calculated on the basis of a reduced-order model of the power system. The reduced-order model is produced on-line by a least-squares identification procedure.

The on-line identifier identifies the discrete transfer function coefficients of a linear approximation to the actual system. The order of the model required depends on the nature of the system being controlled. A low-order model is desirable from the standpoint of the number of computations required for identification and control. In many cases a third-order model is sufficient; successful controller operation has been obtained using a third-order model with simulated power systems of sixteenth order. However in the case of one five-machine system, in which no natural damping was included in any of the five machines, a fifth-order model was required to obtain effective damping [23].

The identifier uses var-unit susceptance as the input signal. The low-order model is recursively fitted using the local bus frequency deviation (deviation from 60 hertz) as the output signal. As the model parameters are identified they are sent along with the latest values of input susceptance and system output to the adaptive observer and the LQG controller. A more detailed description of the controller is contained in the following sections.

Simulation results are presented for the nine bus network used in the previous chapter. The controller is shown to be effective in damping oscillations caused by faults. In one case, with no SVC control applied, a disturbance produces instability in the system; but with the controller in place, stability is restored.
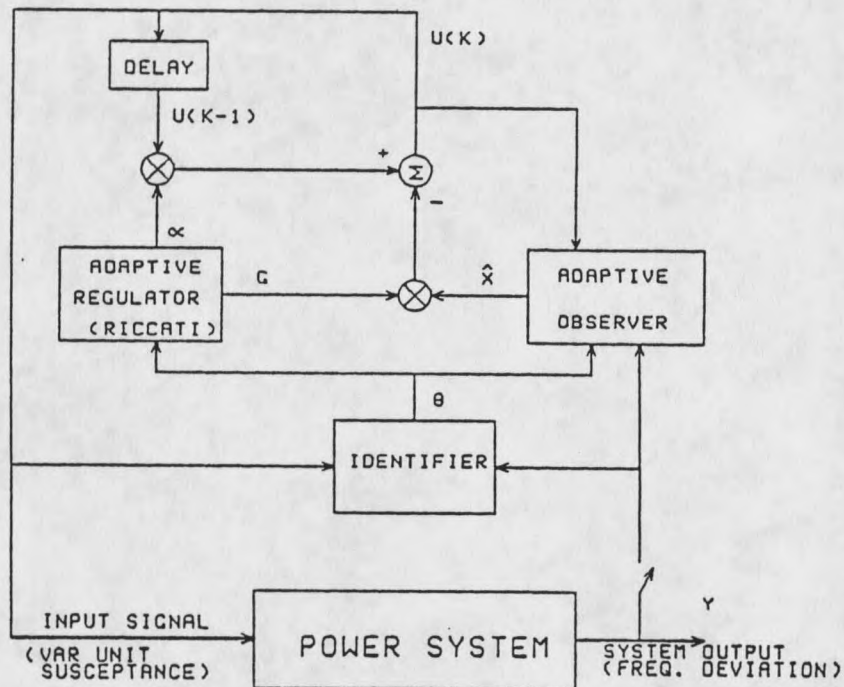
Figure 13. Self-tuning enhanced LQ adaptive control.

An Adaptive LQG Controller

The objective of this section is to present an adaptive linear-quadratic-Gaussian (LQG) control algorithm.   Control is calculated on the basis of a reduced-order model of the power system. The control dampens the output of the system, reducing it to zero; the controller is a self-tuning adaptive regulator.

Consider a dynamic system having output y(k) and input u(k) at periodic sampling instants with k assuming integer values. The input u is updated at periodic sampling instants, with values of u being held constant between sampling instants.   We would like to minimize the following performance measure:

$$J = \sum_k \{ y^2(k) + \lambda_1 u^2(k) + \lambda_2 [u(k)-u(k-1)]^2 \} \qquad (4.1)$$

where the summation is over future sampling instants. The parameter λ_1 > 0 serves as an inverse gain constant. When λ_1 is small, there is little penalty for exerting control, and the gains of the control system tend to be large. Conversely, when λ_1 is large, there is significant penalty for exerting control, and the gains of the control system are small. The parameter λ_2 > 0 serves to temper the rate at which the control can change. When λ_2 is small, little penalty is imposed on erratic swings in the control; but when λ_2 is large, rapid changes in the control are penalized. Standard LQG controllers contain terms corresponding to λ_1. With the addition of the λ_2 term, the controller is an enhanced LQ controller, or an ELQ controller.

The system model used in the ELQ controller is of lower order than the actual system for reasons of decreased computational requirements. The reduced-order system model for the control system is represented as a linear discrete-time transfer function:

$$y = \frac{z^{-1} \bar{B}(z^{-1})}{1 + z^{-1} \bar{A}(z^{-1})} u \qquad (4.2)$$

where

$$\bar{A}(z^{-1}) = a_1 + a_2 z^{-1} + \ldots + a_n z^{-n+1} \qquad (4.3)$$

$$\bar{B}(z^{-1}) = b_1 + b_2 z^{-1} + \ldots + b_n z^{-n+1} \qquad (4.4)$$

and

$$z^{-1} y(k) = y(k-1) \qquad (4.5)$$

In regard to the model (4.2), the ELQ adaptive controller is very tolerant and is insensitive to the following: 1) nonminimum phase zeros and poles; 2) common roots in the numerator and denominator polynomials; and 3) zero values of leading b_i coefficients. It is assumed, however, that unstable modes of the system are observable and controllable.

Equation (4.2) also can be written as

$$y(k) = \phi^T(k-1) \; \theta \tag{4.6}$$

where

$$\theta^T = [a_1 \; \cdots \; a_n \; b_1 \; \cdots \; b_n] \tag{4.7}$$

and

$$\phi^T(k-1) = [-y(k-1) \; \cdots \; -y(k-n) \; u(k-1) \; \cdots \; u(k-n)] \tag{4.8}$$

or, in an observable-canonical state form [43], [44],

$$x(k+1) = Ax(k) + Bu(k) \tag{4.9}$$

$$y(k) = C \; x(k) \tag{4.10}$$

with

$$A = S + KC \; ; \; B^T = [\; b_1 \; \cdots \; b_n \;] ; \; K^T = [\; -a_1 \; \cdots \; -a_n \;];$$

$$C = [\; 1 \; 0 \; \cdots \; 0 \;] \quad \text{and}$$

$$S = \begin{bmatrix} 0 & 1 & 0 & \cdots & & 0 \\ 0 & 0 & 1 & \cdots & & 0 \\ & & & \ddots & & \cdot \\ \cdot & & & & \ddots & \cdot \\ \cdot & & & & & 0 \\ \cdot & & & & & 1 \\ 0 & & \cdots & & & 0 \end{bmatrix} \tag{4.11}$$

so that

$$A = \begin{bmatrix} -a_1 & 1 & 0 & \cdots & 0 \\ -a_2 & 0 & 1 & & \vdots \\ & & & \ddots & 0 \\ \vdots & & & & 1 \\ -a_n & \cdot & \cdot & \cdot & 0 \end{bmatrix} \qquad (4.12)$$

It is this observable-canonical state form that is used in the subsequent development.

As indicated in Figure 13 the three parts of the adaptive control are the identification, the adaptive observer, and the calculation of control. Each of these components of control is discussed below.

Parameter Identification

Let $\theta(k)$ denote the estimation of the parameter vector at time k. To identify θ, recursive identification is used because it is easily implemented on computers. The recursive algorithm used in this paper is discussed in more detail in another section. Continuous estimation of the parameter vector is required because of the variation of power system parameters with system conditions and because a low-order model is being used to represent a high-order system. The power system parameters that are identified are used in both the adaptive observer and in the calculation of control.

Adaptive Observer

The objective of an observer is the estimation or reconstruction of inaccessible states of a system. Usually states are inaccessible because they cannot be measured by transducers for one reason or another. In the case of a reduced-order observer, the observer states do not have a one-to-one correspondence to actual system states. With the observer, fictitious states are created that can be used to form the control $u(k)$ and to produce an observer output that is an approximation to the real, measured output of the system. Control of the system is formulated as control of the observer, which is normal for observer-based systems. To estimate these fictitious states, a low-order adaptive observer is used. It is directly based on the observable-canonical equations (4.9)-(4.12) of the system. It receives parameters from the identifier, which makes it adaptive. The equations are

$$\hat{x}(k+1) = A\hat{x}(k) + Bu(k) + K(k)(y(k) - \hat{y}(k).) \qquad (4.13)$$

$$\hat{y}(k) = C \hat{x}(k) \qquad (4.14)$$

where $A = A(\theta,k)$; $B = B(\theta,k)$; $C = [1\ 0\ \dots\ 0]$;
and $\hat{x}(k)$ is the reduced-order state vector. The matrices A and B are formed using the outputs of the parameter identification procedure, as is indicated below equation (4.10). The gain vector $K(k)$ is the same as that given below (4.10) for the special case of a finite-settling-time observer.

The error between the system and the observer is given by

$$\epsilon(k) = y(k) - \hat{y}(k) \qquad\qquad (4.15)$$

The objective of the observer is to drive the error (4.15) between the system and the observer to zero, so that controlling the observer will be equivalent to controlling the power system.

In the coding of the observer, the observable-canonical form of equations is taken advantage of, to reduce the number of calculations required.

Calculation of Control

A cost function similar to that of (4.1), but for a finite-time problem, is

$$J = x^T(N)Qx(N) + \lambda_2 u^2(N-1) + \sum_{k=i}^{N-1} \{x^T(k)Qx(k) - 2u(k)\lambda_2 u(k-1)$$

$$+ u^2(k-1)\lambda_2 + u^2(k)[\lambda_1 + \lambda_2]\} \qquad (4.16)$$

where $Q = C^T C$ because $y = Cx$. By considering a new state, $v(k+1) = u(k)$, and augmenting the state vector and the state equations accordingly, the state-space representation of the system becomes

$$\tilde{x}(k+1) = \begin{bmatrix} x(k+1) \\ -- \\ v(k+1) \end{bmatrix} = \begin{bmatrix} A & | & 0 \\ -- & | & -- \\ 0 & | & 0 \end{bmatrix} \begin{bmatrix} x(k) \\ -- \\ v(k) \end{bmatrix} + \begin{bmatrix} B \\ -- \\ 1 \end{bmatrix} u(k) \quad (4.17)$$

The cost function (4.16) now can be rewritten in the form

$$J = \tilde{x}^T(N)\tilde{S}\tilde{x}(N) + \sum_{k=i}^{N-1} \{\tilde{x}^T(k)\tilde{Q}\tilde{x}(k) + 2\tilde{x}^T(k)\tilde{M}u(k) + u^2(k)\tilde{\lambda}\} \qquad (4.18)$$

where $\quad \tilde{S} = \begin{bmatrix} Q & 0 \\ \hline 0 & 0 \end{bmatrix} \qquad \tilde{Q} = \begin{bmatrix} Q & 0 \\ \hline 0 & \lambda_2 \end{bmatrix} \qquad \tilde{M} = \begin{bmatrix} 0 \\ \hline -\lambda_2 \end{bmatrix}$

and $\qquad \tilde{\lambda} = (\lambda_1 + \lambda_2)$

This cost function fits a standard form for the LQ control problem [45], [46], for which the calculation of optimal control inputs involves the solution of a discrete Ricatti equation.

Another approach [23] which is essentially equivalent, utilizes dynamic programing to minimize a cost function of the form

$$\min_{u(k)'s} \sum_{k=i}^{N} \{x^T(k)Hx(k) + \lambda_1 u^2(k) + \lambda_2 [u(k) - u(k-1)]^2\}$$

$$= x^T(i)R_i x(i) + s_i u^2(i-1) + 2u(i-1)x^T(i)q_i \qquad (4.19)$$

where the nxn matrix R_i, the nx1 vector q_i, and the scalar s_i satisfy discrete Riccati equations. Bellman's principle of optimality is applied using (4.9) and (4.19), to obtain the optimal feedback control law

$$u(k) = \alpha_k u(k-1) - G_k^T x(k) \qquad (4.20)$$

where α_k and G_k are computed iteratively using the appropriate Riccati equations. The Riccati terms R, q, and s, are solved backwards in k

starting with initial values at k = N of

$$R_N = H = C^T C \tag{4.21}$$

$$q_N = [\ 0\ 0\ \ldots\ 0\ ]^T \tag{4.22}$$

and

$$s_N = \lambda_1 \lambda_2 / (\ \lambda_1 + \lambda_2\ ) \tag{4.23}$$

New values of α_k, G_k, R_k, q_k, and s_k, along with an auxiliary vector V_k and auxiliary vector β_k, are computed using the following sequenced equations starting with k = N-1 and continuing back to k = i :

$$V_k = R_{k+1} B + q_{k+1} \tag{4.24}$$

$$\beta_k = \lambda_1 + \lambda_2 + s_{k+1} + B^T(V_k + q_{k+1}) \tag{4.25}$$

$$G_k = A^T V_k / \beta_k \tag{4.26}$$

$$\alpha_k = \lambda_2 / \beta_k \tag{4.27}$$

$$R_k = C^T C + A^T R_{k+1} A - \beta_k G_k^T G_k \tag{4.28}$$

$$s_k = (1 - \alpha_k)\lambda_2 \tag{4.29}$$

and

$$q_k = \lambda_2 G_k \tag{4.30}$$

The matrices A, B, and C are the same as those used in the observer. These parameters are transmitted from the identification routine and vary as the power system varies. If this were not the case the

calculation of the gains derived from the Riccati equations could be done off-line.

The performance measure (4.1) is for an infinite horizon problem; the appropriate Riccati solution in that case is the steady-state Riccati solution which can be obtained from (4.24) to (4.30) by allowing i to approach $-\infty$, or by iterating the equations until steady-state values of α and G are obtained. For adaptive control, another approach is required in order to limit the number of calculations performed during each control period. A typical adaptive approach is as follows. After initial parameter estimates have been obtained, but before adaptive control is applied, equations (4.24) through (4.30) are iterated once per control period for a set number of control periods, say 30 such periods. Next, adaptive control actions are calculated using the most recent values of α and G, and the resulting control is applied while (4.24) through (4.30) continue to be iterated just once per control period. Also, because the actual x(k) state of the system is not available for use in (4.20), it is replaced by the state $\hat{x}$ of the observer. The observer calculations can be executed in parallel with the Riccati calculations.

The resulting adaptive control signal that is found is suboptimal because:

(1) The model of the system is a linearized model of a nonlinear system.

(2) The model of the system is of lower order than the actual system.

(3) The Riccati equations (4.24) through (4.30) are iterated only once during each sample period.

and

(4) The observer state x̂ is used in place of the actual state x(k) in calculating the feedback control.

Recursive Parameter Identification

In the last several years numerous algorithms for system parameter identification have been developed. Among these algorithms the recursive least squares (RLS) and its extensions are the most popular. Improving computational efficiency, enhancing numerical stability, and avoiding unnecessary storage are key factors influencing the design and implementation of real-time recursive least squares identification algorithms. One can improve both accuracy and computational efficiency by applying UD factorization techniques in the updating of the covariance matrix [47],[48].

The basic assumption inherent in the use of this identification algorithm is that a mathematical model of the dynamic, time-invariant, single-input/single-output process can be described by a generalized linear regression equation of the form

$$y(k) = -a_1 y(k-1) - a_2 y(k-2) - \ldots -a_{na} y(k-na)$$
$$+ b_1 u(k-1) + b_2 u(k-2) + \ldots + b_{nb} u(k-nb)$$
$$+ n(k) \tag{4.31}$$

where u is the plant input variable, y is the plant output variable and n represents the error term (n is a combination of noise, bias, and

plant modeling error). The above equation can be represented as a vector equation,

$$y(k) = \theta^T(k)\phi(k-1) + n(k) \qquad (4.32)$$

where the parameter vector θ is defined in equation (4.7) and the data or regressor vector ϕ is defined in equation (4.8). The objective of identification is to determine the parameter vector, $\theta(k)$, from the sequence of inputs and outputs which form the data vector.

In order to avoid unneccesary storage space the one-dimensional version of the UD algorithm is used. This algorithm is included in reference [48].

Two commonly encountered problems with RLS type algorithms both involve the covariance matrix. The problems with the covariance matrix are:

(1) The trace of the covariance matrix can become too large when there is not enough excitation or richness in the in-coming data. This can occur whenever a constant value for the forgetting factor is used.

(2) The trace of the covariance matrix can become very small making the identifier insensitive to changes in the system being identified. This can occur when a good fit of the data has been obtained but then the system being identified suddenly changes. Then because of the low value of covariance, the identifier gives little weight to incoming information, and parameter updates are too slow.

These problems can be overcome by making two modifications to the standard UD algorithm. The first modification is to reset the covariance matrix whenever the trace goes above or below some specified limits [49]. The reset value of the covariance matrix typically equals 10^6 times the identity matrix. The second modification is to recalculate the forgetting factor at each time step to maintain an almost constant trace for the covariance matrix as suggested in [50]. These modifications have both been implemented to obtain the results presented in this thesis.

Power System Simulation and Modeling

The effectiveness of the above controller has been tested by computer simulation of different power systems. The power systems are the same as described in Chapter 3. Exciters are modeled but not governors. Loads are represented as constant admittances. Results are presented for the nine-bus network with two generators and an infinite bus. Data for this power system is contained in Table 1.

Each machine is represented by seven state variables. Four of these state variables represent machine parameters: rotor angle, time derivative of rotor angle, direct-axis transient voltage, and quadrature-axis transient voltage. Three more state variables represent parameters of the IEEE type I exciter model [35]: output voltage of the forward amplifier, applied field voltage, and output voltage of the feedback compensator.

The system output used for control is a filtered version of local bus frequency. The filter is a bandpass filter which blocks the DC component of the local bus frequency and also attenuates frequency components above the common swing modes. This minimizes any subsynchronous resonance interaction and also provides a relatively smoothly varying signal suitable for fitting to a linear transfer function. The circuit diagram and transfer function for this filter have been presented in Chapter 3. The corner frequencies of this filter are set at 0.05 and 5.0 hertz. The measurement of local bus frequency deviation is simulated by measurement of the bus voltage relative angle at the beginning of the sample period (but after the control or var-unit susceptance has been changed) and again at the end of the sample period. The change in this angle divided by the elapsed time period is then passed through the bandpass filter to become the output signal of the system. Two state variables are used in simulating the bandpass filter.

In order to facilitate the identification of the parameters of the transfer function in (4.2) a probing signal is used. The probing signal is a preselected sequence of var-unit susceptance values that are chosen to excite the presumed natural modes of the power system. The probing signal used in these simulations is a pseudo-random telegraph wave. This means that the var-unit susceptance will switch back and forth between a positive and negative value at pseudo-random time intervals. The magnitude of the probing signal is kept as small as possible so as not to over-excite modes that may have been already excited by a disturbance. The probing signal is used whenever some

disturbance or change in the power system has occurred and the reduced-order model needs to be updated before any control action is taken.

A summary of the way the program executes is as follows: Every 0.1 seconds during the simulation (the sampling period) the identifier receives a value of the output y and the input u which has been applied to the system for the past sample period. It then calculates a new set of coefficients for the reduced-order transfer function model. These coefficients are passed to the adaptive observer and the adaptive ELQ controller. The observer calculates a new state vector estimate, and the controller calculates a new set of feedback gains. The gains are calculated by iterating the Riccati equations once during each sample period. The control action is then computed to give the next susceptance value of the var unit. The network algebraic equations are solved using this value of susceptance over the next sample period. This results in an approximate solution to the minimization of a quadratic cost function. The controller and identifier are both executed at a sampling period of 0.1 seconds while the Runge-Kutta integration proceeds at a time step of .01 to .001 seconds. Whenever a disturbance or other change in the power system has occurred, a probing signal is used to facilitate parameter identification before the ELQ control is applied to the system. The computer code used to simulate the adaptive controller, including the Riccati calculations and the adaptive observer, is contained in Appendix D.

Simulation Results

A three-phase to ground fault has been simulated at the midpoint of transmission line 5-7 to create a disturbance. The fault lasts for three cycles beginning at $t = 0.1$ seconds. The line is then disconnected at both ends for 6 cycles before reclosing back in. The network is then back to its original state at $t = 0.25$ seconds.

The system response to this disturbance with the var unit dynamic control disabled is presented in Figures 14 and 15. The input and output signals (var-unit susceptance and filtered bus frequency deviation) are shown in Figure 14, while the machine rotor angles are shown in Figure 15. The machines both experience poorly damped oscillations at two frequencies. One is near 1.1 Hz and the other is near 0.14 Hz. The existence of both modes has been verified by eigenvalue analysis. The higher frequency oscillation occurs when the damping coefficients in the swing equations are set to zero. The lower frequency mode appears when the exciter models are included in the simulation.

The system response with the var-unit dynamic control enabled is illustrated in Figures 16 and 17. In this simulation the probing signal starts as soon as the line is reclosed at 0.25 seconds and it continues until $t = 1.5$ seconds at which time the ELQ control is applied to the system. When the probing signal begins the parameter vector and observer state vector are both zero so the controller is not

starting with any information about the system prior to the disturbance.

The weights being used in this simulation are $\lambda_1 = 2.0$ and $\lambda_2 = 2.0$. The figures illustrate that the var unit dampens the 1.1 Hz oscillation very rapidly while driving the output signal to zero. The two machines, however, are still oscillating at the lower frequency. The output signal, frequency deviation, approximates a derivative of the voltage angle signal which tends to de-emphasize the lower frequency signal components compared to the higher ones. This, along with the smaller magnitude of the lower mode, causes no discernable deviation to appear in the output signal for the lower mode.

To illustrate the effect of changing the weighting factors, the same disturbance is simulated again but with $\lambda_1 = 2,000.0$ and $\lambda_2 = 2.0$. The results are illustrated in Figures 18 and 19. Although the results are similar to those in Figures 16 and 17 in many ways, a close inspection of the curves will show a difference in the var-unit susceptance and in the time it takes to dampen the oscillations in the output signal. Increasing the value of λ_1 causes the control signal to not vary as much away from zero so that the var unit does not reach its maximum or minimum values, and the oscillation takes longer to dampen out.

In Figures 20 and 21 the same disturbance is simulated with weighting factors of $\lambda_1 = 2.0$ and $\lambda_2 = 5,000.0$. It can be seen that the major effect of increasing λ_2 is to produce a smoother variation in the var-unit susceptance along with a decrease in the overall size of the control action.

In order to study the effectiveness of the var unit in damping out more than one oscillatory mode, a different disturbance is used. This disturbance consists of disconnecting line 4-5 from the network with no reclosing, thus forcing to system to seek a new equilibrium point. The system response to this disturbance with the var unit disabled is shown in Figures 22 and 23. This disturbance also causes two oscillatory modes to appear, but this time both frequencies are present in the output signal. It is also interesting to note that the system seems to be unstable at this new operating point. Line disconnection takes place at $t = 0.1$ seconds and probing starts at 0.25 seconds and continues until $t=1.5$ seconds. The results with the var unit enabled are shown in Figures 24 and 25, using a third-order identifier model and weights of $\lambda_1 = 2.0$ and $\lambda_2 = 200.0$. The figures illustrate that the controller quickly dampens the higher frequency mode first and then the lower frequency mode. However as the lower frequency mode is dampened the higher frequency oscillation (which is unstable) begins to appear again. This seems to indicate that a third-order model will only be able to work on one oscillatory mode at a time. It also appears that the process of damping the higher frequency oscillation is exciting the lower frequency oscillation and vice versa.

For the sake of comparison the same open line disturbance is run again with the same controller weights but using a fifth-order identifier model. The results of this simulation are presented in Figures 26 and 27. In this simulation the controller is able to dampen both modes simultaneously. It is interesting to note that on the first disturbance with reclosing, successful performance of the controller was very insensitive to the weights used. On this second disturbance

with no reclosing however, varying the weighting factors resulted in significantly different controller responses.

Figures 28 through 30 are from the same simulation illustrated by Figures 16 and 17 where a third-order model is being used to damp out oscillations caused by the short circuit disturbance with reclosing. The identified model parameters are shown in Figures 28 and 29 as they were obtained during the simulation. The estimated value of the output obtained by the observer and the actual output value are shown in Figure 30 to illustrate the tracking of the adaptive observer.
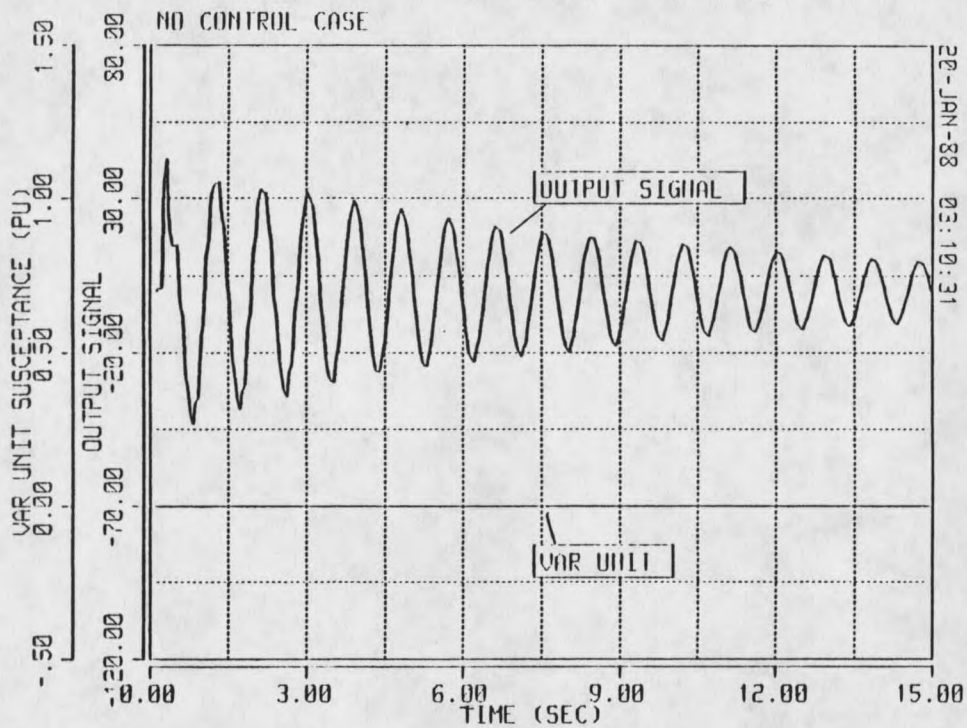
Figure 14. Three-phase fault disturbance, no var unit control. System input and output signals.
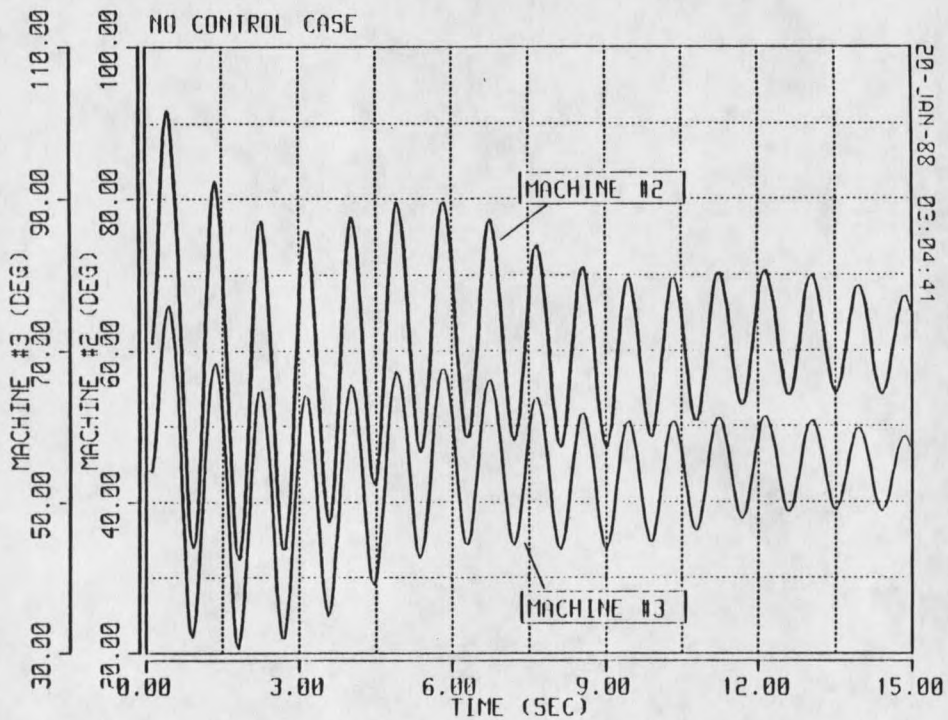
Figure 15. Three-phase fault disturbance, no var unit control. Generator rotor angles.
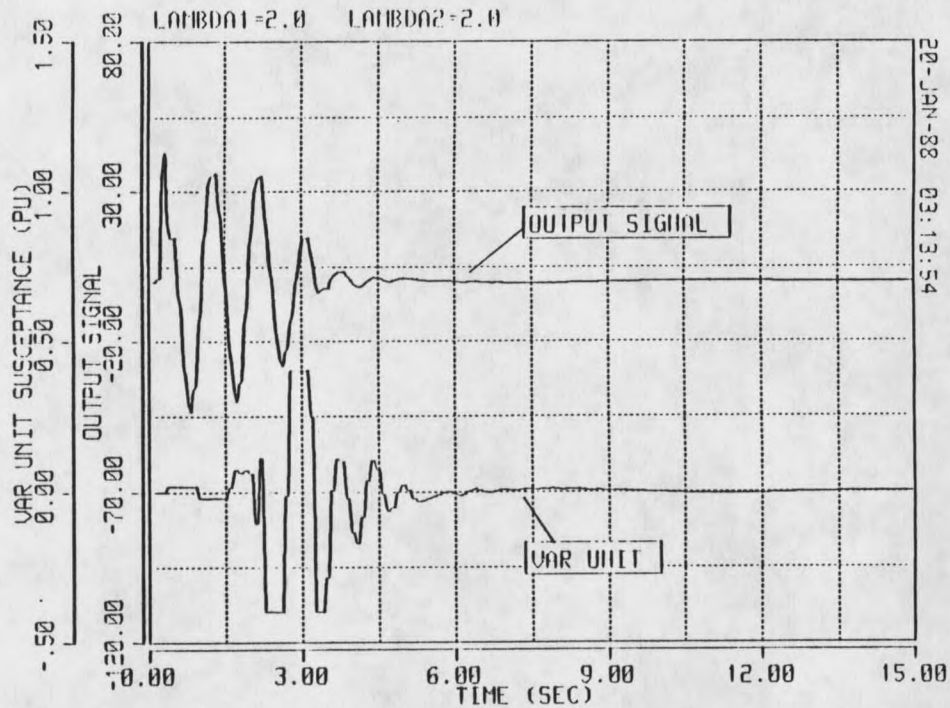
Figure 16. Three-phase fault disturbance, third-order adaptive controller, λ_1 =2.0 , λ_2 = 2.0. System input and output signals.
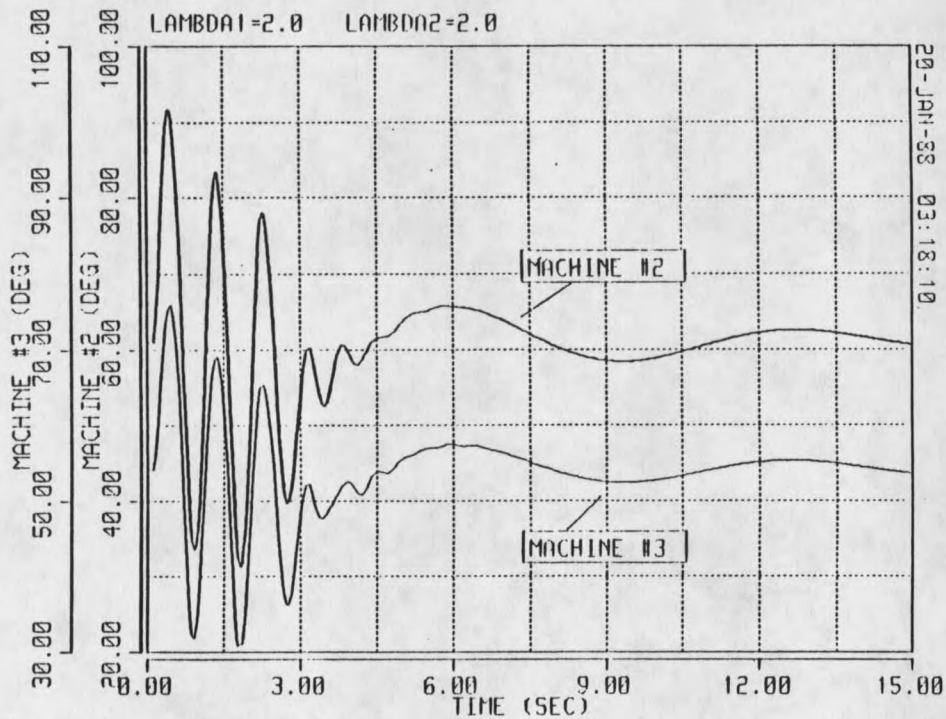
Figure 17. Three-phase fault disturbance, third-order adaptive controller, λ_1 =2.0 , λ_2 = 2.0. Generator rotor angles.
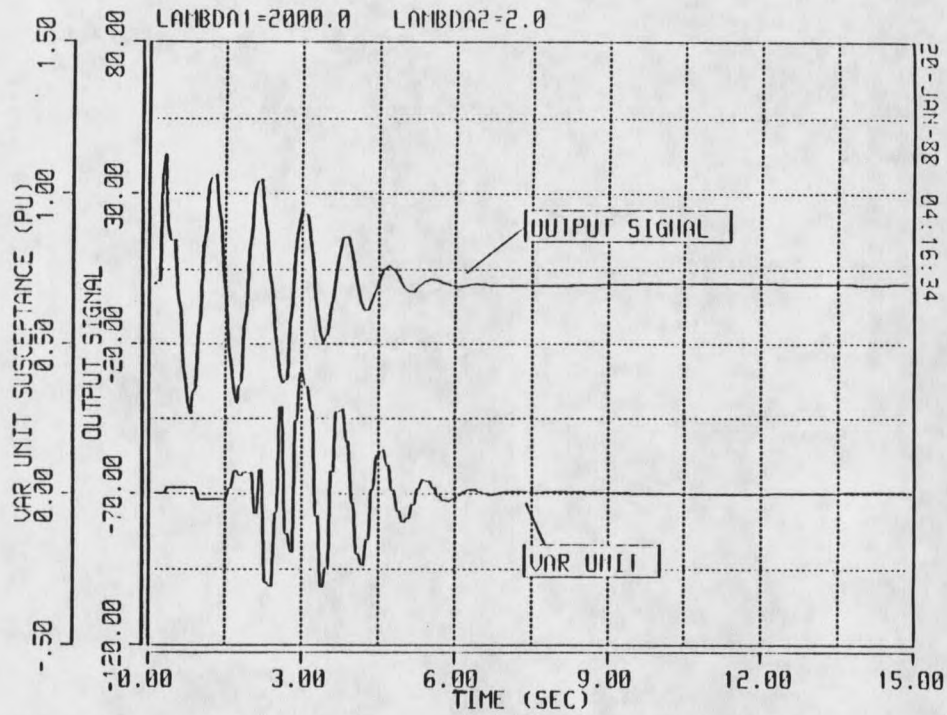
Figure 18. Three-phase fault disturbance, third-order adaptive controller, λ_1 =2000.0 ,λ_2 = 2.0. System input and output signals.
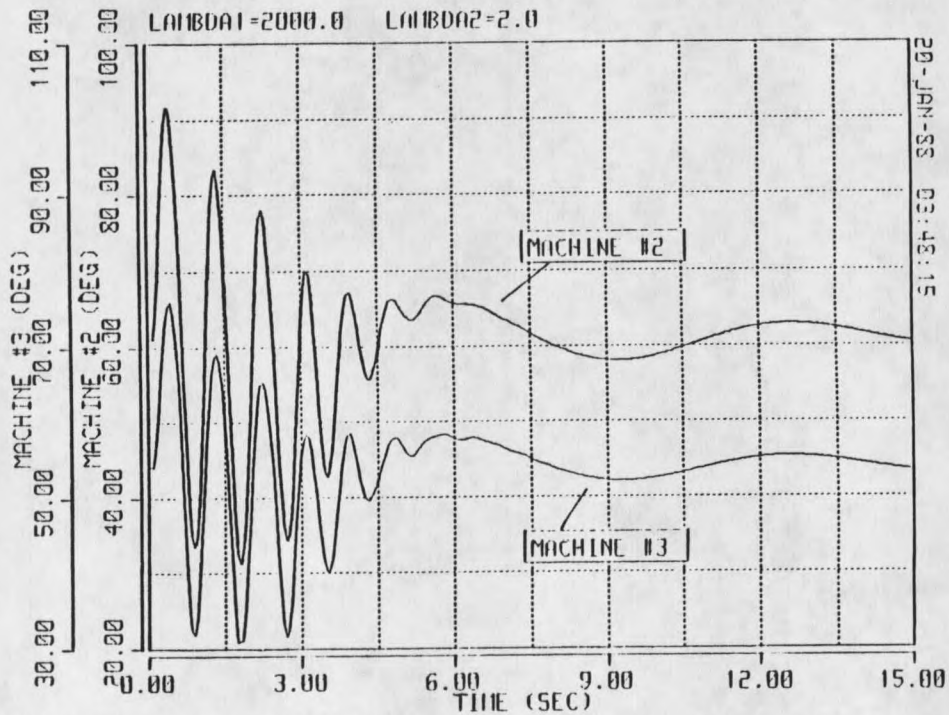
Figure 19. Three-phase fault disturbance, third-order adaptive controller, λ_1 =2000.0 ,λ_2 = 2.0. Generator rotor angles.
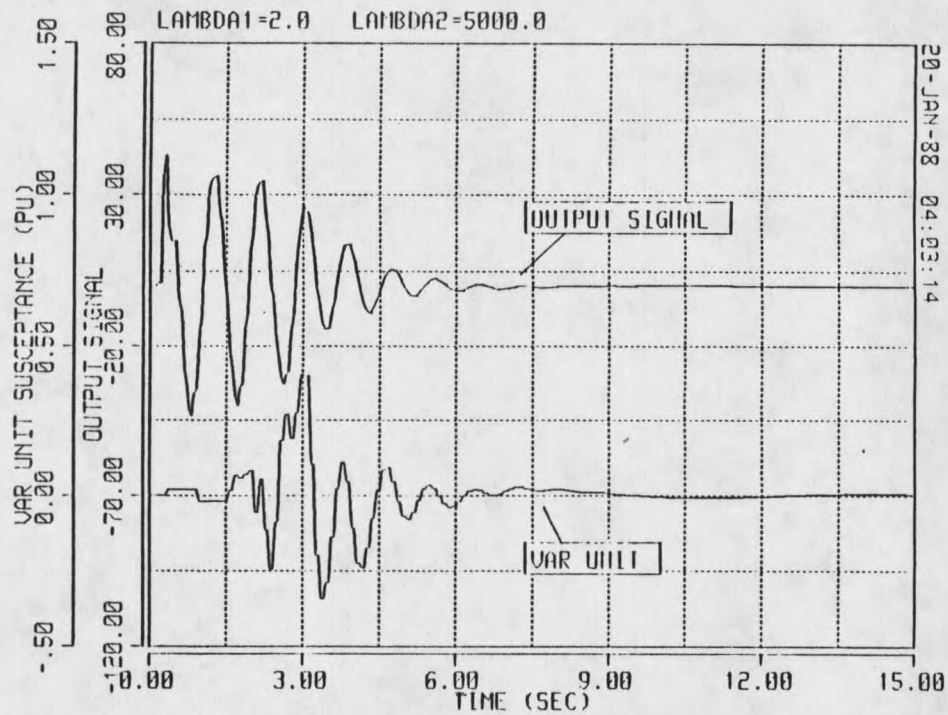
Figure 20. Three-phase fault disturbance, third-order adaptive controller, λ_1 =2.0 , λ_2 = 5000.0. System input and output signals.
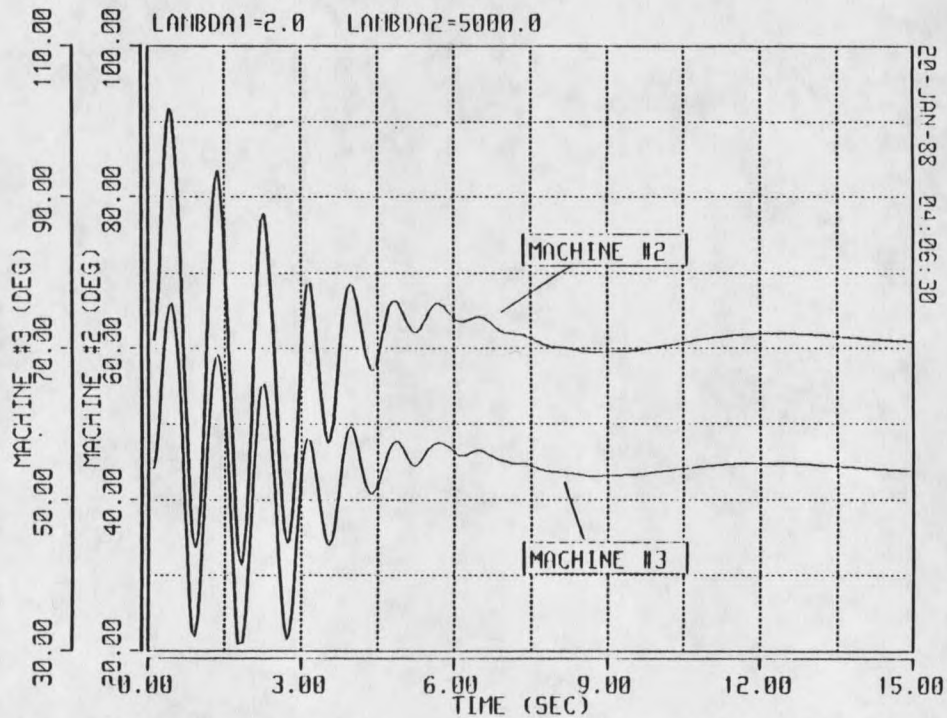
Figure 21. Three-phase fault disturbance, third-order adaptive controller, λ_1 =2.0 , λ_2 = 5000.0. Generator rotor angles.

83
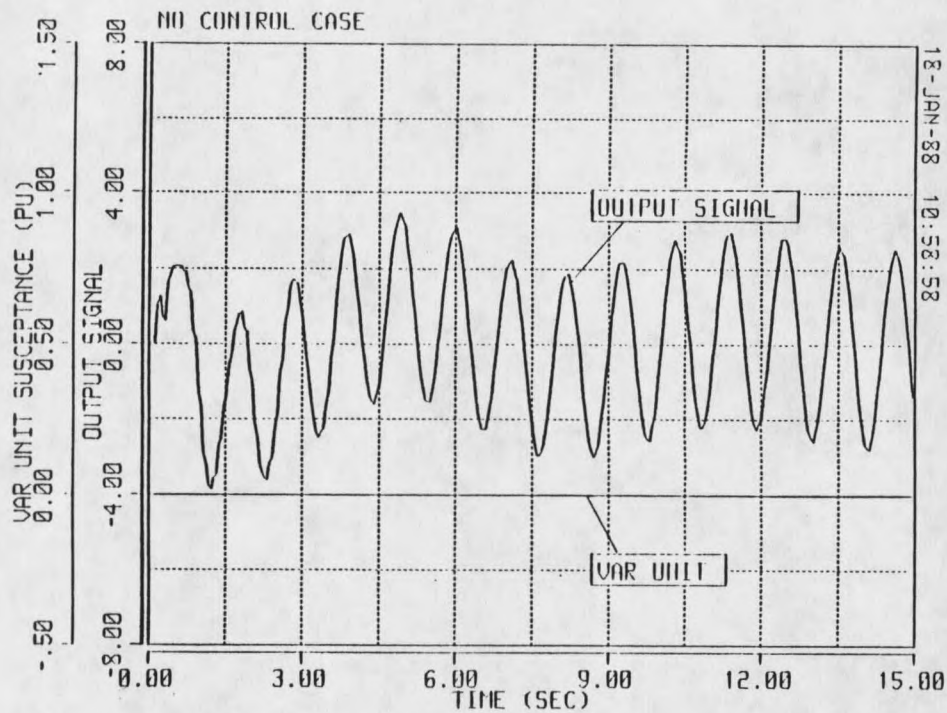
Figure 22. Open-line disturbance, no control case. System input and output signals.
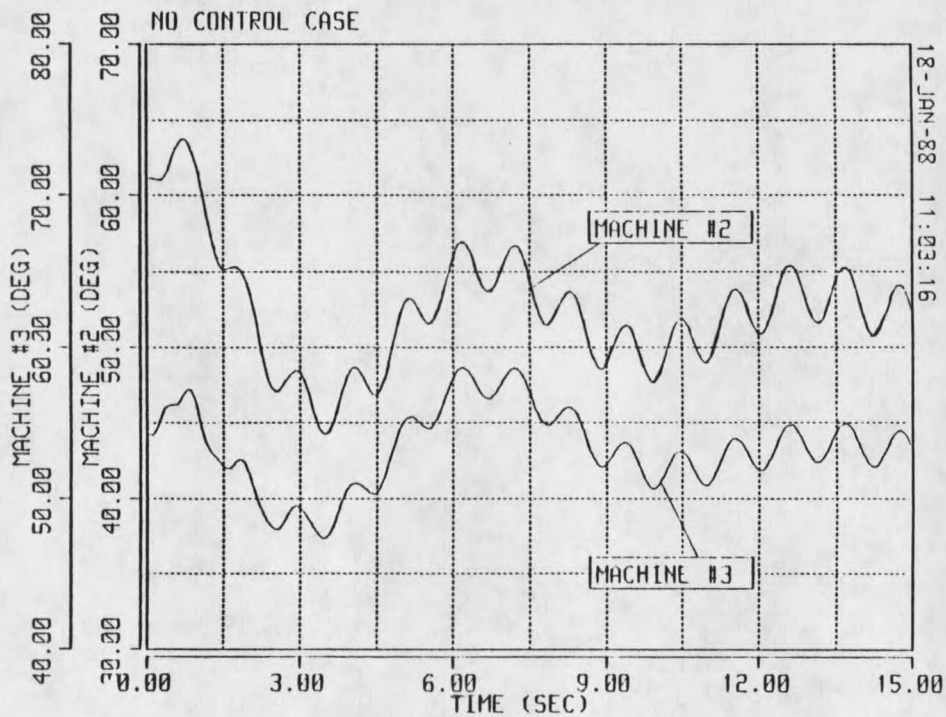
Figure 23. Open-line disturbance, no control case. Generator rotor angles.

84
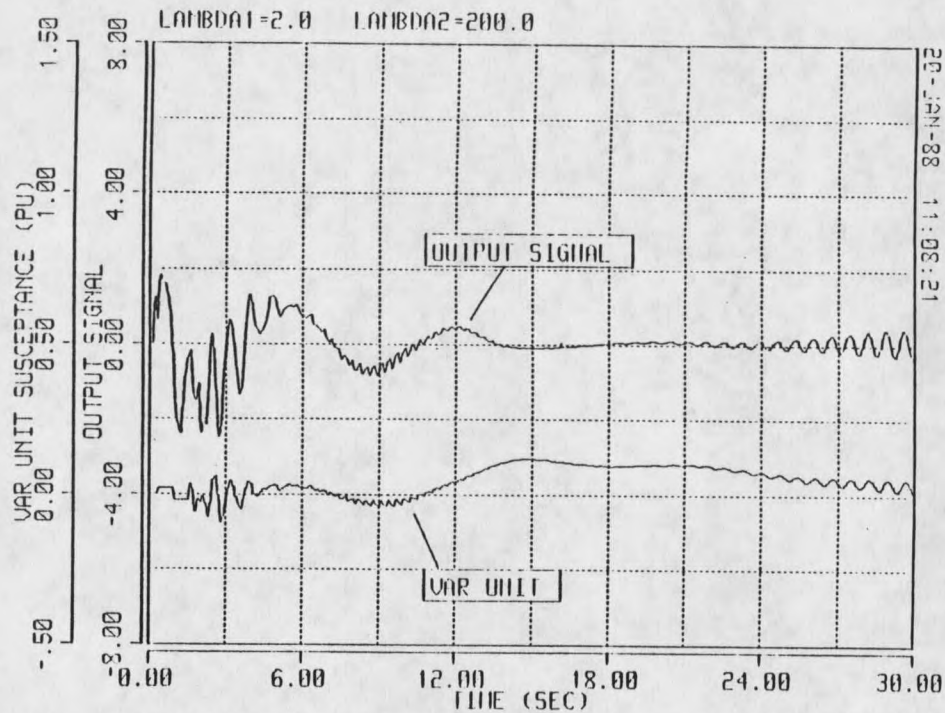
Figure 24. Open-line disturbance, third-order adaptive controller, λ_1 =2.0 , λ_2 = 200.0. System input and output signals.
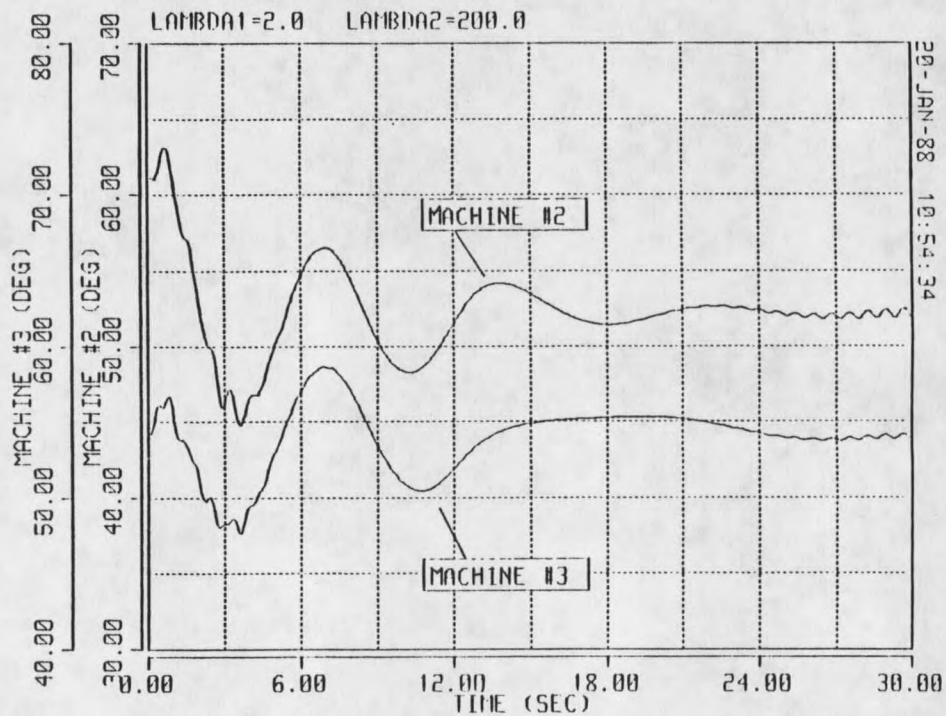
Figure 25. Open-line disturbance, third-order adaptive controller, λ_1 =2.0 , λ_2 = 200.0. Generator rotor angles.
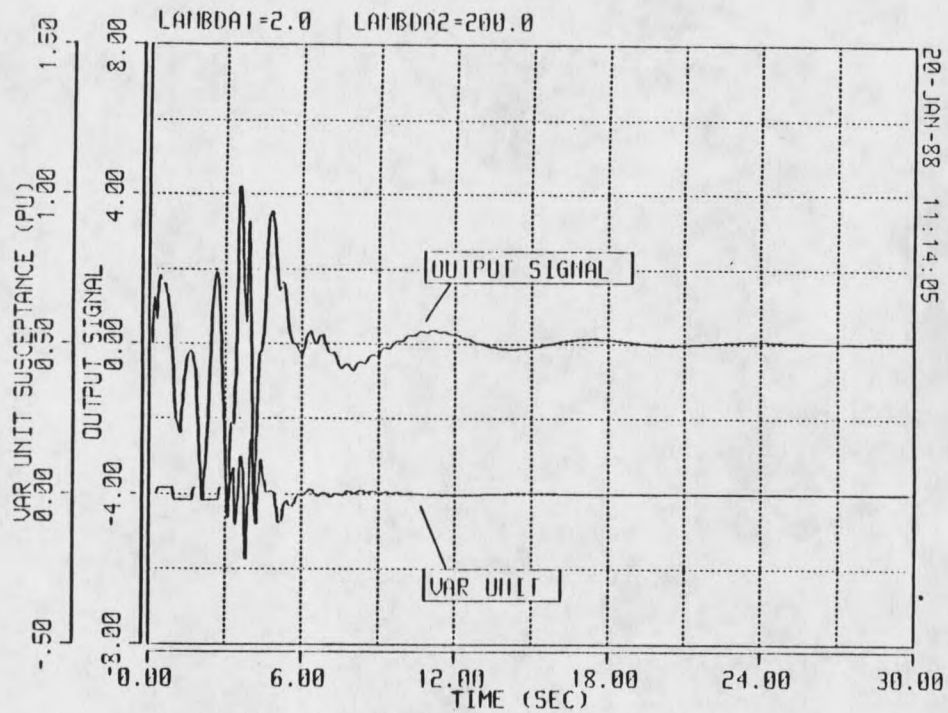
Figure 26. Open-line disturbance, fifth-order adaptive controller, λ_1 =2.0, λ_2 = 200.0. System input and output signals.
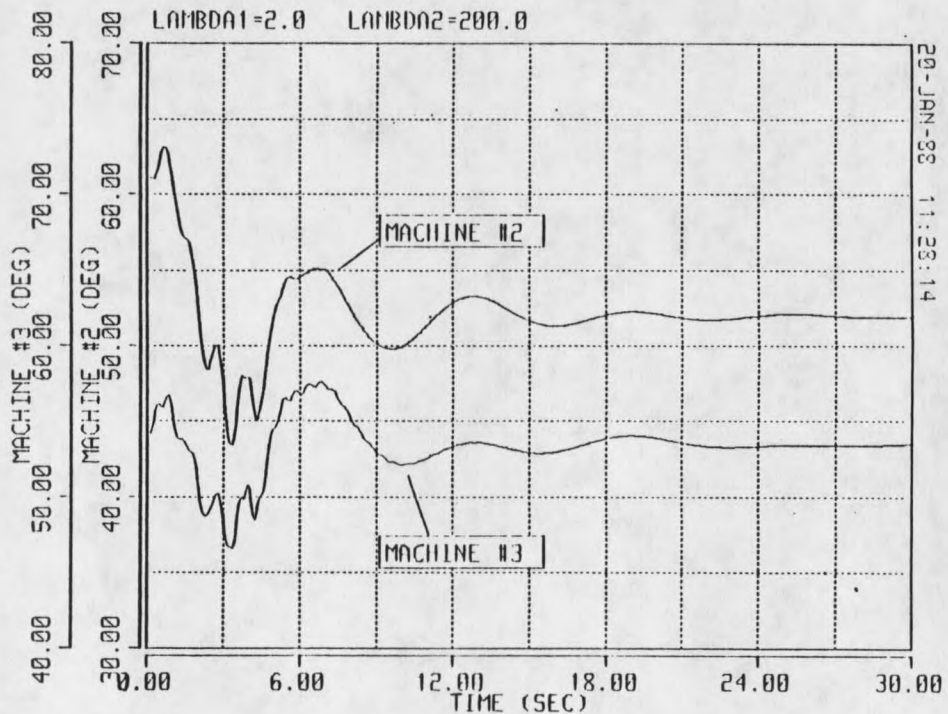
Figure 27. Open-line disturbance, fifth-order adaptive controller, λ_1 = 2.0, λ_2 = 200.0. Generator rotor angles.
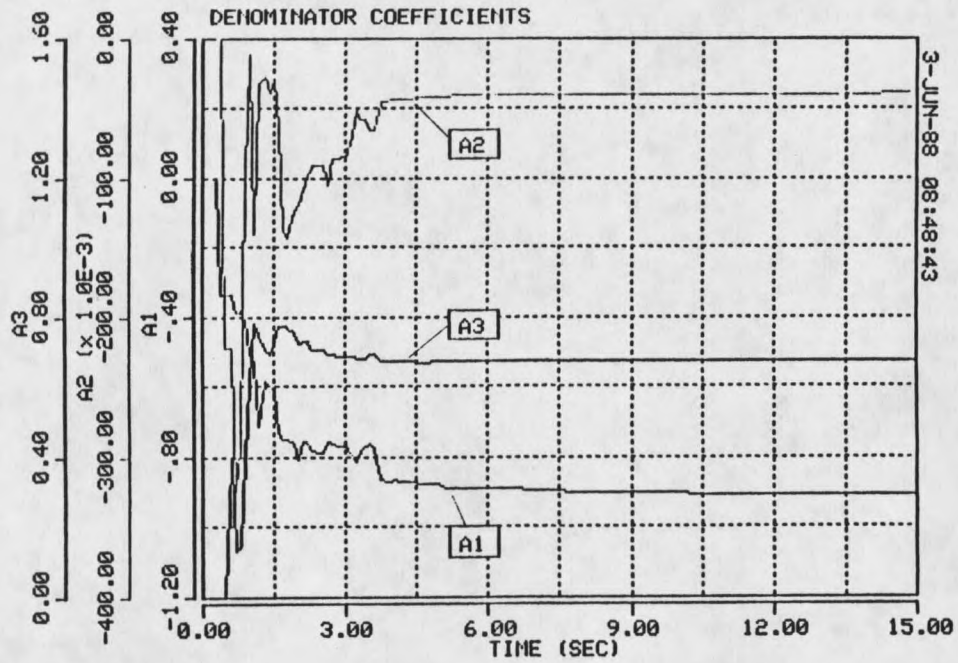
Figure 28. Denominator coefficients of reduced-order identified model for three-phase disturbance.
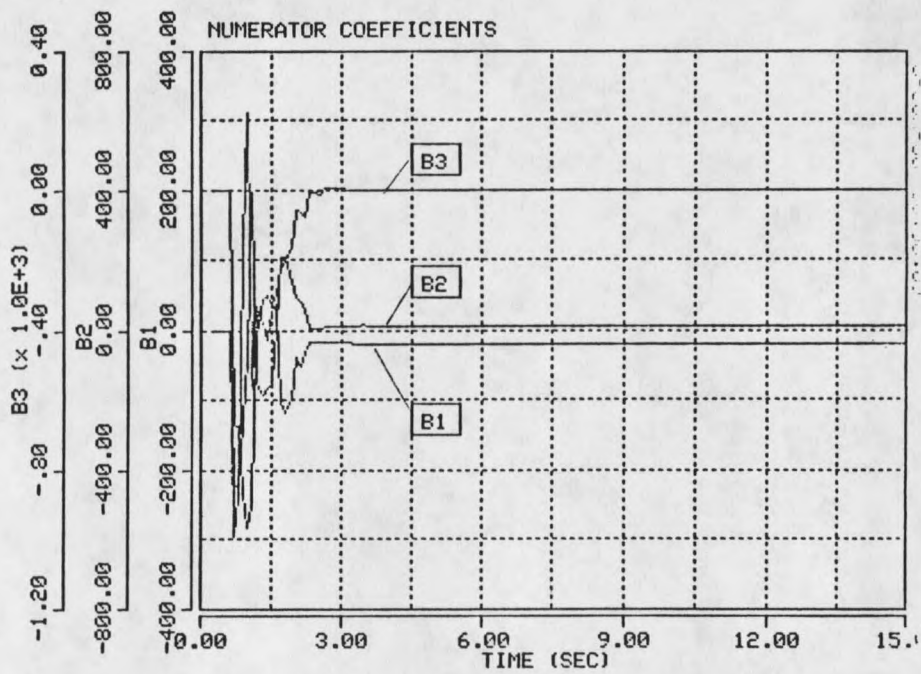
Figure 29. Numerator coefficients of reduced-order identified model for three-phase disturbance.
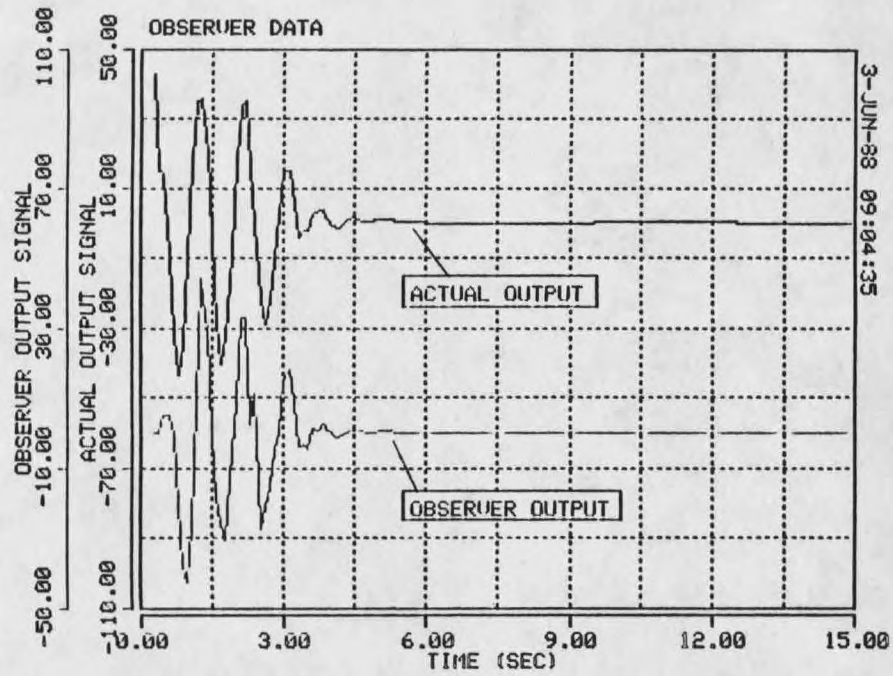
Figure 30. Observer estimate of system output and actual system output signals for three-phase fault disturbance.

CHAPTER 5

CONCLUSION AND FUTURE WORK

General Comments

Two separate approaches to the problem of improving power system damping by designing robust controllers for SVC's have been presented. Both of these methods require only locally measured system signals to control the var unit susceptance in order to dampen machine and system oscillations. The effectiveness of both approaches has been tested by simulation on a nine-bus power system. These simulations illustrate the usefulness and relative strengths of each type of controller, and also the potential for application to very large power systems.

Much work remains to be done however, on either design approach, before it can be concluded that such a controller is suitable to implement on a large power system. An important step among remaining tasks is the need to implement these controllers in computer simulations of power systems containing thousands of buses and hundreds of generators. Simulations of this scale are needed to assess the effectiveness and robustness of the controllers in a realistic system. Software capable of simulating large-scale power systems and accepting flexible and complex control routines has yet to be developed.

Another area warranting further research is the coordination of SVC control with other power system devices such as power system stabilizers or HVDC systems. A logical extension of the work presented

here is to enhance system damping by controlling several SVC's throughout the power network.

The Fixed Controller

In Chapter 3 a nonadaptive controller design strategy has been presented which is based on a computer generated linearized model of the nonlinear system used for simulation of power system dynamics. The linearized model is used to design a fixed feedback controller based on eigenvalue analysis of the closed-loop system. Robustness is incorporated into the design by readjusting controller parameters in consideration of different system operating conditions. The main advantage of this approach is that the controller acts very quickly with no need to adapt and with no problems arising from a failure to adapt. The disadvantages include the need to foresee ahead of time all the possible different operating conditions under which the controller will be acting, and to make sure that the controller functions appropriately for each of these conditions.

It is possible that a large range of operating conditions will result in a very similar set of system eigenvalues, in which case the selection of the proper controller structure may simplify the process of tuning the controller parameters. In general there seems to be a trade-off between robustness and effectiveness for the fixed controller. Proper selection of the controller structure in terms of the number of poles and zeros may help to minimize this trade-off. It is also possible that this type of controller could be made adaptive,

at least in a rudimentary sense, by establishing several different operating regions of the power system and designing a feedback compensator for each. The adaptive strategy would then involve identifyng which operating region the system is currently in and using a table look-up method to determine the proper controller parameters for the fixed compensator. This approach could be feasible if only a few parameters require adjustment, and if the controller is implemented in digital form rather than in the analog form presented in Chapter 3.

The Adaptive Controller

In Chapter 4 a self-tuning adaptive control strategy is presented which has the inherent capability of being more robust than the fixed controller. The adaptive ELQ controller adjusts its control based upon on-line identification of a reduced-order transfer function of the system. The advantage of this type of controller is that the control action is automatically tuned as the system operating conditions change. There is no requirement for off-line analysis of each of the system operating points before the conditions actually occur.

There are still some aspects of the controller that warrant further investigation. One of these aspects is the sensitivity of some operating conditions to the selected values of weighting parameters, λ_1 and λ_2. It was pointed out previously that under some conditions a wide range of parameter settings will result in successful control action while in another case only a very narrow range of parameters

will give acceptable control action. It is possible that this situation may be resolved by calculating the weighting parameters on-line from a measurement of the sensitivity of the system output to changes in var unit susceptance. Another possible solution is to set the parameters at some relatively high value and accept the decreased effectiveness that may result in some operating environments.

Another aspect that warrants some further investigation is the selection of the proper order of the controller that is needed to achieve acceptable performance. The simulations presented here suggest that a system with more lightly damped modes will require a higher order adaptive controller in order to enhance damping of all the modes simultaneously. It has not been demonstrated that the highest-order computationally feasible controller will always give appropriate control actions. In other words if a third-order controller will provide sufficient damping in a certain case, then will a fifth or a seventh-order controller also work? It is possible that the identification of the number of critical system modes can be done in real time with the order of the controller adjusted accordingly.

Also, a thorough investigation into which type of identification routine is best suited for power system applications is needed. The UD routine used here seems to perform very well under most of the conditions tested and it has the advantage of being very computationally efficient. One drawback of this method however is the inherent assumption that all disturbances present in the system output signal can be modeled as white noise. In the power system environment an important situation which needs accurate identification is immediately after a large disturbance. In this situation there is a

large component of the output signal due to the disturbance which is deterministic (a decaying sinsusoid) and not stochastic in nature. Although the UD algorithm seems to converge quite well despite this condition, a better estimate of the reduced-order transfer-function parameters probably could be obtained by a routine that is capable of separating the disturbance component of the output signal from that part of the output which is due to the var unit input. Algorithms which have been developed for this situation are often sensitive to the degree of correlation between the desired output signal and the disturbance signal, and this correlation causes them to be ineffective for power system applications.

The flexibility of being able to change the cost function to tailor the control action of an LQG type of controller for a particular type of application is another advantage of this approach. One potentially useful strategy is to use a multivariable approach where there is one system input and two system outputs so that the cost function contains two output terms. Both outputs are locally measured network signals which are selected to enhance the control effectiveness of the var unit. The ELQ controller is readily modified for the two output case which then requires parallel identifiers and parallel observers, one for each output signal. Preliminary work [51] in this area indicates some benefits in improving the effectiveness of the control action.

REFERENCES CITED

1   Hauer, J. F., "A Perspective on the Need for Robust Damping Controls in the Western U.S. Power System," IEEE Control Systems Magazine, publication pending.

2   Byerly, R. T., D. E. Sherman and D. K. McLain, "Normal Modes and Mode Shapes Applied to Dynamic Stability Analysis," IEEE Trans. on Power Apparatus and Systems, vol. PAS-94, No. 2, March/April 1975, pp. 224-229.

3   Hauer, J. F., "Reactive Power Control as a Means for Enhanced Interarea Damping in the Western U.S. Power System—A Frequency Domain Perspective Considering Robustness Needs," Application of Static Var Systems for System Dynamic Performance, IEEE Special Publication # 87TH0187-5-PWR, 1987, pp. 79-92.

4   Rusche, P. A., D. L. Hackett, D. H. Baker, G. E. Gareis, and P. C. Krause, "Investigation of the Dynamic Oscillations of the Ludington Pumped Storage Plant," IEEE Trans. on Power Apparatus and Systems, Vol. PAS-95, No. 6 November/December 1976, pp. 1854-1862.

5   Van Ness, J. E., F. M. Brasch, G. L. Landgren, S. T. Naumann, "Analytical Investigation of Dynamic Instability Occuring at Powerton Station," IEEE Trans. on Power Apparatus and Systems, Vol. PAS-99, No. 4, July/August 1980, pp. 1386-1395.

6   Mugwanya, D. K., J. E. Van Ness, "Mode Coupling in Power Systems," IEEE Trans. on Power Apparatus and Systems, Vol. PWRS-2, No. 2, May 1987, pp. 264-270.

7   deMello, F. P., and C. Concordia, "Concepts of Synchronous Machine Stability as Affected by Excitation Control," IEEE Trans. on Power Apparatus and Systems, Vol. PAS-88, No. 4, April 1969, pp. 316-329.

8   Wong, D. Y., G. J. Rogers, B. Porretta and P. Kundur, "Eigenvalue Analysis of Very Large Power Systems," Presented at the IEEE Power Engineering Society Winter Meeting, New Orleans, Louisiana, February 1-6, 1987, paper # 87 WM 102-7.

9   Martins, N., "Efficient Eigenvalue and Frequency Response Methods Applied to Power System Small-Signal Stability Studies," IEEE Trans. on Power Systems, Vol. PWRS-1, February 1986, pp. 217-226.

10 Ohyama, T., K. Yamashita, T. Maeda, H. Suzuki and S. Mine, "Effective Application of Static Var Compensators to Damp Oscillations," IEEE Trans. on Power Apparatus and Systems, Vol. PAS-104, No. 6, June 1985, pp. 1405-1410.

11 Hammad, A. E., "Analysis of Power System Stability Enhancement by Static Var Compensators," IEEE Trans. on Power Systems, Vol. PWRS-1, No. 4, November 1986, pp. 222-227.

12 Hammad, A. E., "Applications of Static Var Compensators in Utility Power Systems," _Application of Static Var Systems for System Dynamic Performance_, IEEE Special Publication # 87TH0187-5-PWR, 1987, pp. 28-35.

13 Olwegard, A., K. Walve, G. Waglund, H. Frank and S. Torseng, "Improvement of Transmission Capacity by Thyristor Controlled Reactive Power," _IEEE Trans. on Power Apparatus and Systems_, Vol. PAS-100, No. 8, August 1981, pp. 3930-3937.

14 Hamouda, R. M., M. R. Iravani and R. Hackam, "Coordinated Static Var Compensators and Power System Stabilizers for Damping Power System Oscillations," Presented at the IEEE Power Engineering Society Winter Meeting, New Orleans, Louisiana, February 1-6, 1987, paper # 87 WM 045-8

15 Larsen, E. V. and J. H. Chow, "SVC Control Design Concepts for System Dynamic Performance," _Application of Static Var Systems for System Dynamic Performance_, IEEE Special Publication # 87TH0187-5-PWR, 1987, pp. 36-53.

16 Martin, D. E., "SVC Considerations for System Damping," _Application of Static Var Systems for System Dynamic Performance_, IEEE Special Publication # 87TH0187-5-PWR, 1987, pp. 68-71.

17 Pierre, D. A., "A Perspective on Adaptive Control of Power Systems," _IEEE Trans. on Power Systems_, Vol. PWRS-2, No. 2, May 1987, pp. 387-396.

18 Pierre, D. A., and J. R. Smith, "Alternative Adaptive Control Methods for Power Systems," _Proceedings_ of the IASTED Conference on High Technology in the Power Industry, Bozeman, MT, August 1986, pp. 162-167.

19 Cheng, S. J., Y. S. Chow, O. P. Malik and G. S. Hope, "An Adaptive Synchronous Machine Stabilizer," _IEEE Trans. on Power Systems_, Vol. PWRS-1, No. 3, August 1986, pp. 101-109.

20 Cheng, S. J., O. P. Malik and G. S. Hope, "Damping of Multi-Modal Oscillations in Power Systems Using a Dual-Rate Adaptive Stabilizer," Presented at the IEEE Power Engineering Society 1987 Winter Meeting, New Orleans, Louisiana, February 1-6, 1987, paper # 87 WM 027-6.

21 Chandra, A., O. P. Malik and G. S. Hope, "A Self-Tuning Controller for the Control of Multi-Machine Power Systems," Presented at the IEEE Power Engineering Society 1987 Summer Meeting, San Francisco, California, July 12-17, 1987, paper # 87 SM 452-6.

22 Wu, C. J., and Y. Y. Hsu, "Design of Self-Tuning PID Power System Stabilizer for Multimachine Power Systems," Presented at the IEEE Power Engineering Society Summer Meeting, San Francisco, California, July 12-17, 1987, paper # 87 SM 512-7.

23 Pierre, D. A., "Enhanced LQ Controllers and Adaptive Control," Electronics Research Laboratory Report No. 687, Montana State University, Bozeman, MT, Nov. 1987.

24 Smith, J. R., D. A. Pierre, D. A. Rudberg, and R. M. Johnson, "Robust Var Unit Control Strategies to Enhance Damping of Power System Oscillations," Proceedings, IASTED Conference on High Technology in the Power Industry, March 1988.

25 Smith, J. R., D. A. Pierre, D. A. Rudberg, I. Sadighi, A. P. Johnson, and J. F. Hauer, "An Enhanced LQ Adaptive Var Unit Controller for Power System Damping," Accepted for presentation at the IEEE Power Engineering Society Summer Meeting, Portland, OR, July 1988.

26 Hsu, Y. Y. and C. J. Wu, "Adaptive Control of a Synchronous Machine Using the Auto-Searching Method," Presented at the IEEE Power Engineering Society Winter Meeting, New York, New York, January 31 - February 5, 1988, paper # 88 WM 169-5.

27 Chow, J. H. and J. J. Sanchez-Gasca, "Frequency Response Evaluation of State Space Designed Controllers for Systems with Lightly Damped Oscillatory Modes - A Power System Stabilizer Example," Proceedings of the 26th Conference on Decision and Control, Los Angeles, California, December 1987, pp. 866-872.

28 Petkovski, D. B. and M. Athans, "Robust Decentralized Control of Multiterminal DC/AC Power Systems," Electic Power Systems Research, Vol. 9, 1985, pp. 253-262.

29 Johnson, R. M., "An Interactive State Space Integration Program with Graphics for the Solution of Differential Equations with Constraints," Proceedings, 1982 IEEE Summer Computer Simulation Conference, Houston, TX, July 1982.

30 Stott, B., "Power System Dynamic Response Calculations," Proceedings of the IEEE, Vol. 67 No. 2, February 1979, pp. 219-241.

31 Arrillaga, J., C. D. Arnold and B. J. Harker, Computer Modelling of Electrical Power Systems, John Wiley and Sons, Inc., New York, 1983.

32 Anderson, P. M., and A. A. Fouad, Power System Stability and Control, Iowa State University Press, Ames, Iowa, 1977.

33 Kimbark, E. W., Power System Stability: Vol III, John Wiley and Sons, Inc., New York, 1956.

34 DeMello, F. P., and L. N. Hannett, "Validation of Synchronous Machine Models and Determination of Model Parameters from Tests," IEEE Transactions on Power Apparatus and Systems, Vol. PAS-100 No. 2, 1981, pp. 662-672.

35 IEEE Committee Report, "Computer Representation of Excitation Systems," IEEE Transactions on Power Apparatus and Systems, Vol. PAS-87, June 1968, pp. 1460-1464.

36 Dommel, H. W., and N. Sato, "Fast Transient Stability Solutions," IEEE Transactions on Power Apparatus and Systems, Vol. PAS-91 No. 4, July/August 1972, pp. 1643-1650.

37 Kundur, P., and P. L. Dandeno, "Implementation of Advanced Generator Models into Power System Stability Programs," IEEE Transactions on Power Apparatus and Systems, Vol. PAS-102 No. 7, 1983, pp. 51-56.

38 Armstrong, E. S., ORACLS: A Design System for Linear Multivariable Control, Marcel Dekker, Inc., New York, 1980.

39 Samson, C., "An Adaptive LQ Controller for Nonminimum-Phase Systems," International J. Control, Vol. 35, No. 1, pp. 1-28, 1982.

40 Clarke, D. W., P. P. Kanjilal, and C. Mohtadi, "A Generalized LQG Approach to Self-Tuning Control, Part I. Aspects of Design," International J. Control, Vol. 41, No. 6, pp. 1509-1523, 1985.

41 Clarke, D. W., P. P. Kanjilal, and C. Mohtadi, "A Generalized LQG Approach to Self-Tuning Control, Part II. Implementation and Simulation," International J. Control, Vol. 41, No. 6, pp. 1525-1544, 1985.

42 M'Saad, M., M. Duque, and I. D. Landau, "Practical Implications of Recent Results in Robustness of Adaptive Control Schemes," Proceedings, IEEE Conference on Decision and Control, Athens, Greece, pp. 477-481, Dec. 1986.

43 Franklin, G. F., and J. D. Powell, Feedback Control of Dynamic Systems, Addison-Wesley Pub. Co., Reading, Mass., 1986.

44 D'Azzo, J. J., and C. H. Houpis, Linear Control System Analysis and Design, Conventional and Modern, McGraw-Hill Book Co., New York, 1981.

45 Dorato, P., and A. H. Lewis, "Optimal Linear Regulators: The Discrete-Time Case," IEEE Transactions on Automatic Control, Vol. AC-16, No. 6, December, 1971, pp. 613-620.

46 Kuo, B. C. Digital Control Systems, SRL Publishing Company, Champaign, Illinois, 1977.

47 Bierman, G. J., and C. L. Thornton, "Filtering and Error Analysis via the UDU Covariance Factorization," IEEE Trans. on Automatic Control, Vol. AC-23, 1987, pp. 901-907.

48 Clarke, D. W., "Some Implementation Considerations of Self-Tuning Controllers," pp. 81-110 of Numerical Techniques for Stochastic Systems, edited by F. Archetti and M. Cugiani, North Holland Publishing Co., New York, 1980.

49 Goodwin, G. C., and K. S. Sin, Adaptive Filtering, Prediction and Control, Prentice Hall, Englewood Cliffs, New Jersey, 1984.

50 Sripada, N. R., and D. G. Fisher, "Improved Least Squares Identification for Adaptive Controllers," Proceedings, American Control Conference, Mineapolis, MN, pp. 2027-2037, June 1987.

51 Pierre, D. A., "Power System Damping: A Simulation Program and Enhanced LQ Self-Tuning Strategies," for the June 20-22 1988 International Workshop on Adaptive Control Strategies for Industrial Use, Alberta, Canada.

APPENDICES

APPENDIX A

SUBROUTINES FOR SIMULATION OF POWER SYSTEM DYNAMICS

Both subroutines in this appendix are called by INTEG, A Runge-Kutta integration package. STATE is called four times for each integration step while SIDE is called only once at the end of each integration step.

```
************************************************************
      SUBROUTINE STATE(X,DX,T,DT,N)
      IMPLICIT NONE
      INTEGER FLAG,N,I,J,K
      REAL*8 DX(1),X(1),T,DT,EF1,EF2,XD1,XD2,XDP1,XDP2,XQ1,XQ2
      REAL*8 XQP1,XQP2,TDOP1,TDOP2,TQOP1,TQOP2,MG1,MG2,RA1,RA2
      REAL*8 KA1,KA2,TA1,TA2,KF1,KF2,TF1,TF2,KE1,KE2,TE1,TE2
      REAL*8 RA3,XD3,XDP3,XQ3,XQP3,TDOP3,TQOP3,MG3,KA3,TA3
      REAL*8 KF3,TF3,KE3,TE3
      REAL*8 WO,YR,YM,PI

      COMMON/IMPED/XQ1,XQ2,XQ3,XQP1,XQP2,XQP3,XD1,XD2,XD3,
     &          XDP1,XDP2,XDP3,RA1,RA2,RA3

C*********************************************************************
C        STATE VARIABLES OF THE SYSTEM:

C    X(1) = W--- ROTOR VELOCITY
C    X(2) = DELTA --- ROTOR ANGLE
C    X(3) = EQP Q AXIS INTERNAL VOLTAGE
C    X(4) = EDP D AXIS INTERNAL VOLTAGE
C    X(5) = VA --- OUTPUT OF FORWARD PATH BLOCK ON EXCITER MODEL
C    X(6) = EF  -- EXCITER FIELD VOLTAGE
C    X(7) = VF --FEEDBACK LOOP ON EXCITER
C    X(8) --- LIST STARTS OVER -- ROTOR VELOCITY MACHINE #2
C
C     SIDE VARIABLES OF THE SYSTEM
C
C    X(N+1) = PE--ELEC PWR        X(N+10) = PM--MECH PWR
C    X(N+2) = ID                  X(N+11) =SEF1--SAT FACTOR(NOT USED)
C    X(N+3) = IQ                  X(N+12) =SEV1--SAT FEEDBACK VOLT
C    X(N+4) = VQ                  X(N+13) = VREF1--EXITER SET POINT
C    X(N+5) = VD                  X(N+14) = MAG OF VT
C    X(N+6) = VR --RE(VT)         X(N+15) = (UNUSED)
C    X(N+7) = VIM--IM(VT)         X(N+16) = LIST STARTS OVER- PE2
C    X(N+8) = IR --TERM CURR      X(N+17) = ID (MACHINE #2 ETC)
C    X(N+9) = IIM                 X(N+18) =
C*********************************************************************
      DATA XQ1 ,XQP1/0.0969,0.0969/XD1,XDP1/0.1460,0.0608/
     & TDOP1,TQOP1/8.96,0.001/RA1/0.00/KA1,TA1/40.,.06/
     &     KF1,TF1/.04,.715/KE1,TE1/-.05,.5/
```

Figure 31. Subroutines for simulation of power system dynamics.

```
      DATA XQ2,XQP2/0.8645,0.1969/XD2,XDP2/0.8958,0.1198/
     & TDOP2,TQOP2/6.00,0.53/RA2/0.00/KA2,TA2/25.0,0.2/
     &     KF2,TF2/.091,.35/KE2,TE2/-.0505,.5685/
      DATA XQ3,XQP3/1.2578,0.25/XD3,XDP3/1.3125,0.1813/
     &TDOP3,TQOP3/5.89,0.600/RA3/0.00/KA3,TA3/25.,.2/
     &     KF3,TF3/.105,.350/KE3,TE3/-.0582,.6544/
      PI = 4.00*DATAN(1.00D+00)
      WO = 2.0*60.0*PI
      MG1 = 23.64/(PI*60.0)
      MG2 = 6.40/(PI*60.0)
      MG3 = 3.01/(PI*60.0)
      IF (T .EQ. 0.0D00) THEN
         X(N+46) = 180.0*X(2)/PI
         X(N+47) = 180.0*X(9)/PI
         X(N+48) = 180.0*X(16)/PI
      ENDIF

C     *******************************************
C     NOTE THAT THE STATE EQUATIONS FOR MACHINE #1 HAVE BEEN SET TO ZERO
C     IN ORDER TO REPRESENT IT AS AN INIFINITE BUS.
C     *******************************************

C     DX(1) = (1.D0/(MG1))*(X(N+10) - X(N+1))
      DX(1) = 0.D0
C     DX(2) =  X(1)-WO
      DX(2) = 0.D0
C     DX(3) = (X(6) + (XD1 - XDP1)*X(N+2) - X(3))/TDOP1
      DX(3) = 0.0
C     DX(4) = (-(XQ1 - XQP1)*X(N+3) - X(4))/TQOP1
      DX(4) = 0.0
C     DX(5) = (X(N+13)*KA1 - X(N+14)*KA1 - X(7)*KA1 - X(5))/TA1
      DX(5) = 0.0
C     DX(6) = (X(5) - X(N+12) - X(6)*KE1)/TE1
      DX(6) = 0.0
C     DX(7) = (KF1/(TF1*TE1))*(X(5) - X(N+12) - X(6)*KE1) - X(7)/TF1
      DX(7) = 0.0
C     ***********************************
      DX(8)  =  (1.D0/(MG2))*(X(N+25) - X(N+16))
      DX(9)  =  X(8)-WO
      DX(10) =  (X(13) + (XD2 - XDP2)*X(N+17) - X(10))/TDOP2
      DX(11) =  (-(XQ2 - XQP2)*X(N+18) - X(11))/TQOP2
      DX(12) =  (X(N+28)*KA2 - X(N+29)*KA2 - X(14)*KA2 - X(12))/TA2
      DX(13) =  (X(12) - X(N+27) - X(13)*KE2)/TE2
      DX(14) =  (KF2/(TF2*TE2))*(X(12)-X(N+27)-X(13)*KE2)-X(14)/TF2
C     ***********************************
      DX(15) =  (1.D0/(MG3))*(X(N+40) - X(N+31))
      DX(16) =  X(15)-WO
      DX(17) =  (X(20) + (XD3 - XDP3)*X(N+32) - X(17))/TDOP3
      DX(18) =  (-(XQ3 - XQP3)*X(N+33) - X(18))/TQOP3
```

Figure 31 - continued.

```
      DX(19) =  (X(N+43)*KA3 - X(N+44)*KA3 - X(21)*KA3 - X(19))/TA3
      DX(20) =  (X(19) - X(N+42) - X(20)*KE3)/TE3
      DX(21) =  (KF3/(TF3*TE3))*(X(19)-X(N+42)-X(20)*KE3)-X(21)/TF3
C  ***********************************************
C    NOTE THAT THESE LAST TWO STATE EQUATIONS REPRESENT THE FILTER
C    IN THE CASE OF THE ADAPTIVE CONTROLLER OR THE COMPENSATOR IN THE
C     CASE OF THE FIXED CONTROLLER

      DX(22) = 10.0*PI*(X(N+50)-X(22))
      DX(23) = (10.0*PI*(X(N+50)-X(22))) - X(23)*0.01*PI


      RETURN
      END
C
C
      SUBROUTINE SIDE(X,DX,T,DT,N)
      IMPLICIT NONE
      INTEGER ITR,I,J,K,FLAG,N,NA,NB,IGO,ISTART,m
      INTEGER FFLG,NAV,TICK,TICK2,nc,nd
      REAL*8 X(1),DX(1),T,DT,RA1,RA2,XD1,XD2,XDP1,XDP2,XQ1,XQ2,XQP1,XQP2
      REAL*8 XOLD(100),DIFF(100),K12,K22,K13,K23,EPS,ALPHA,SLOPE,ERR
      REAL*8 EFMX2,EFMX3
      REAL*8 RA3,XD3,XDP3,XQ3,XQP3
      REAL*8 SE75MX2,SEMX2,SE75MX3,SEMX3,CSIG,WO,VINFMAG,XSS(50),G(10)
      REAL*8 TIMER,MARK,WTF,WTP,FREQ,TC,OLDANG2,FREQ2
      REAL*8 XLAMBDA,QUAL,THETA(100),TRACE,ERROR,UDUM,PI
      REAL*8 CON,PDIAG,TMARK1,UNEXT,THAV(100),THDAT(100,100)
      REAL*8 DFAC,DELD1,DELD2,DELD3,ANG1,ANG2,ANG3,ANG8,OLDANG8
      REAL*8 OLDDEL1,OLDDEL2,OLDDEL3,MARK2,TIMER2,TOTITR,TOTCYC
      REAL*8 AVGITR,FREQ8,ANGDIFF,SSANG8
      REAL*8 trace_ab,trace_cd,estv
      COMPLEX*16 VOLT1,VOLT2,VOLT3,CUR1,CUR3,Y11,Y14,Y22,Y27,Y33
      COMPLEX*16 VOLT4,VOLT5,VOLT6,VOLT7,VOLT8,VOLT9,CUR2
      COMPLEX*16 Y39,Y44,Y45,Y46,Y55,Y57,Y66,Y69,Y77,Y78,Y88,Y89,Y99
      COMPLEX*16 EINF,EINFSS,IMPED1

      COMMON/IMPED/XQ1,XQ2,XQ3,XQP1,XQP2,XQP3,XD1,XD2,XD3,
     &          XDP1,XDP2,XDP3,RA1,RA2,RA3

      DATA SE75MX2,SEMX2/0.0778,0.303/,EFMX2/3.96/
      DATA SE75MX3,SEMX3/0.0895,0.349/,EFMX3/3.438/


      PI = 4.00*DATAN(1.00D+00)
      WO = 2.0*60.0*PI

      DATA Y11,Y14/(0.0,-17.361113),(0.0,17.361113)/
     &       Y22,Y27/(0.0,-16.000),(0.0,16.000)/
```

Figure 31 - continued.

```
&        Y33,Y39/(0.0,-17.064846),(0.0,17.064846)/
&        Y44,Y45,Y46/(3.307379,-39.308891),(-1.365188,11.604095),
&                                     (-1.942191,10.510682)/
&        Y55,Y57/(3.813787,-17.842628),(-1.187604,5.975134)/
&        Y66,Y69/(4.101848,-16.133476),(-1.282009,5.588245)/
&        Y77,Y78/(2.804727,-35.445614),(-1.617123,13.697979)/
&        Y88,Y89/(3.741186,-23.642391),(-1.155087,9.784270)/
&        Y99/(2.437097,-32.153862)/

C    THE FOLLOWING SECTION INITIALIZES THE NETWORK VOLTAGE VALUES
     IF (T .EQ. DT) THEN
        VOLT1 = DCMPLX(1.04,0.0)
        VOLT2 = DCMPLX(1.011527109317,.1656439116)
        VOLT3 = DCMPLX(1.0215533214885,.083986971345)
        VOLT4 = DCMPLX(1.025,-.03938)
        VOLT5 = DCMPLX(.9936,-.06948)
        VOLT6 = DCMPLX(1.0108,-.06537)
        VOLT7 = DCMPLX(1.02386,.06621)
        VOLT8 = DCMPLX(1.015924,.0124125)
        VOLT9 = DCMPLX(1.03137,.036016)
        SSANG8 = DATAN2(DIMAG(VOLT8),DREAL(VOLT8))

C    THESE STATEMENTS INITIALIZE THE INFINITE BUS VALUES
        CUR1 = DCMPLX(0.68846153846,-0.2596153846)
        IMPED1 = DCMPLX(0.0D0,XQ1)
        EINFSS = VOLT1 + CUR1*IMPED1

     ENDIF

C *** CODE FOR SIMULATING DISTURBANCES-- 3 PHASE FAULT W/ RECLOSING
C *** THE ADMITTANCE MATRIX CHANGES ARE CALCULATED AS FOLLOWS
C       Y77FAULTED = Y77 - Y57
C       Y77OPEN = Y77 + Y57
C       Y55FAULTED = Y55 - Y57
C       Y77OPEN = Y77 + Y57
C ***

     IF ((T .GE. 0.10D0) .AND. (T .LE. 0.150D0)) THEN

        Y77 = DCMPLX(2.804727,-35.445614)-DCMPLX(-1.187604,5.975134)
        Y55 = DCMPLX(3.813787,-17.842628)-DCMPLX(-1.187604,5.975134)
        Y57 = DCMPLX(0.0,0.0)
     ELSEIF ((T .GT. 0.15) .AND. (T .LE. 0.25D0)) THEN

        Y77 = DCMPLX(2.804727,-35.445614)+DCMPLX(-1.187604,5.975134)
        Y55 = DCMPLX(3.813787,-17.842628)+DCMPLX(-1.187604,5.975134)
        Y57 = DCMPLX(0.0,0.0)

     ELSE
```

Figure 31 - continued.

```
         Y57 = DCMPLX(-1.187604,5.975134)
         Y77 = DCMPLX(2.804727,-35.445614)
         Y55 = DCMPLX(3.813787,-17.842628)

      ENDIF

C
C
      IF (T .EQ. DT) THEN
         open(unit=14,file='iden.out',status='new')
         open(unit=15,file='obs.out',status='new')
         open(unit=16,file='LQG.out',status='new')
C        open(unit=17,file='CONT.out',status='new')
         OPEN(UNIT=17,FILE='MISC.INF',STATUS='NEW')
C        OPEN(UNIT=20,FILE='',STATUS='NEW')
C
         write(14,790) 6
 790     format(/,' identifier coef ',/,2x,i2)
C
         write(15,792) 6
 792     format(/,' observer data ',/,2x,i2)
C
         write(16,794) 6
 794     format(/,' LQG DATA ',/,2x,i2)
C
         write(17,796) 5
 796     format(/,' CONTROL DATA--pdiag,tr-ab,tr-cd,estv,
     &                            csig',/,2x,i2)

C        WRITE(17,798) 5
C 798    FORMAT(/,'    FILT-IN,OUT,MAG,ANG8 ',/2X,I2)
C
C        write(20,799) 6
C 799    format(/,' THAV coef ',/,2x,i2)

C        CSIG = 0.0
         qual = 0.0
         FLAG = 0
      ENDIF

C  *** CODE TO DERIVE A FEQUENCY SIGNAL (POWER IS NOT BEING USED)
C  *** WTP AND WTF ARE WEIGHT FACTORS TO WEIGHT  POWER AND FREQUENCY
C  *** SIGNALS WHICH COULD BE ADDED AND USED AS THE OUTPUT SIGNAL
      WTP = 0.0
      WTF = 10.0

C  **** SET COUNTERS AND CALL IDENTIFICATION AND CONTROL ROUTINES
      TICK = 0
```

Figure 31 - continued.

```
        TICK2 = 0
        TIMER = T-MARK
        TIMER2 = T-MARK2

        IF ((FFLG .EQ. 1) .AND. (TIMER .GE. .05D0 )) THEN
            TMARK1 = T
            FFLG = 0
        ENDIF

C **** CODE FOR A POWER AND FREQ SIGNAL
        IF (TIMER .GE. 0.1D0) THEN
            MARK = T
            TICK = 1
            FFLG = 1
            TC = T-TMARK1
            FREQ8 = (ANG8 - OLDANG8)/(TC-DT)

            X(N+50) = WTF*(FREQ8) + WTP*(x(10)-XSS(10))

            OLDANG8 = ANG8

        ENDIF
        IF (TIMER2 .GE. 1.0D0) THEN
            MARK2 = T
            TICK2 = 1
        ENDIF
        ANGDIFF = ANG8-SSANG8


C **** END OF COUNTER AND TIMER AND FREQ SECTION AND
C **** BEGINNING OF CONTROL SECTION TO FIND A VALUE FOR VAR UNIT C ****
SUSCEPTANCE

C **** THE FOLLOWING LINE IF USED WILL BYPASS ALL CONTROL ACTIONS
C **** don't worry this is the only 'go to' in the whole program !!!!
C    IF (T .GT. DT) GO TO 810

        IF ((TICK .EQ. 1) .AND. (T .GT. 0.25D0)) THEN
                NA = 5
                NB = NA
                XLAMBDA = 0.97
                ISTART = 1
                IF (FLAG .EQ. 0) THEN
                    ISTART = 0
                    FLAG = 1
                ENDIF

C *** THIS 'IF' STATEMENT CONTAINS THE SECTION WHICH CALLS THE
C *** IDENTIFIER -- IT CAN BE USED TO SKIP CALLING THE IDENTIFIER
```

Figure 31 - continued.

```
C  *** BUT STILL CALL THE CONTROL SECTION THUS FREEZING THE C  ***
COEFFICIENTS OF THE IDENTIFIED TRANSFER FUNCTION

            IF (T .LE. 50.DO) THEN
            CSIG = UNEXT
C  *** ANY OF A NUMBER OF IDENTIFICATION ROUTINES CAN BE USED HERE BY
C  *** UNCOMMENTING THE APPROPRIATE LINE.  THE UD IDENTIFIER WORKS MUCH
C  *** BETTER THAN THE OTHERS IN SIMULATIONS DONE SO FAR (6/88).
            PDIAG = 1.0D6
            CALL UUD(CSIG,X(23),XLAMBDA,NA+NB,NA,NB,
            &    ISTART,QUAL,THETA,TRACE,PDIAG)


C           nc = na-1
C           nd = na
C           pdiag = 100.0
C           call ivaml(theta,x(23),csig,na,nb,nc,nd,xlambda,
C     &               trace_ab,trace_cd,pdiag,istart,estv,igo)


CC          PDIAG = 1.0
CC          CON = 1700.0
CC          CALL ILS(CSIG,X(23),XLAMBDA,(NA+NB),NA,NB,
CC    &          ISTART,QUAL,THETA,TRACE,CON,PDIAG)

CC          CALL RLS(T,THETA,X(23),CSIG,NA,NB,(NA+NB),
CC    &         XLAMBDA,ISTART)

      ENDIF

C  *** THIS ENDS THE SECTION OF CODE CALLING THE IDENTIFIER
C  *** 'IGO' IS A FLAG USED TO SIGNAL THE CONTROL ROUTINE TO RETURN A
C  *** PROBING SIGNAL(IGO=1) OR A CONTROL SIGNAL (IGO=2).  IT ALSO CAN
C  *** BE USED TO RETURN A PROBING SIGNAL WITHOUT ITERATING THE RICCATI
C  *** EQUATIONS OR CALCULATING THE OBSERVER STATES (IGO=0).
            IF ( T .LT. 1.0) THEN
               IGO = 1
            ELSEIF ((T .GE. 1.0) .AND. (T .LT. 5.0D0)) THEN
               IGO = 1
            ELSEIF (T .GE. 5.0D0 ) THEN
               IGO = 2
            ENDIF
      CALL CONTROL(THETA,QUAL,X(23),CSIG,NA,IGO,UNEXT,T)
      WRITE(14,802) T,(THETA(I),I=1,6)
 802  FORMAT(7(1X,1PE10.3))
      WRITE(17,803) T,pdiag,trace_ab,trace_cd,estv,CSIG
 803  FORMAT(6(1X,1PE10.3))
C     WRITE(20,804) T,(THAV(I),I=1,6)
C 804 FORMAT(7(1X,1PE10.3))
```

Figure 31 — continued.

```
C  *** THIS STATEMENT IS COMMENTED OUT SO THAT THE SIMULATION WILL HAVE
C  *** A DELAY IN IT CORRESPONDING TO AN ACTUAL IMPLEMENTATION
C          CSIG = UNEXT

C  *** 'QUAL' IS A QUALITY FACTOR WHICH WAS ORIGINALLY BEING USED TO
C  *** TRY TO DETERMINE WHEN THE IDENTIFIER HAD CONVERGED -- IT IS NO
C  *** LONGER AN ESSENTIAL CALCULATION BUT PERHAPS OF SOME VALUE.

          IF ( DABS(X(23)) .LT. 1.0E-02) THEN
             QUAL = 1.0
          ELSE
             QUAL = 1.0 - DABS(ERROR/X(23))
          ENDIF
          IF (QUAL .LT. 0.0) QUAL = 0.0

C  *** THE FOLLOWING STATEMENTS LIMIT THE VAR UNIT TO +- 0.4
          IF (CSIG .LT. -0.4D0) CSIG = -0.4
          IF (CSIG .GT. 0.4D0)  CSIG = 0.4

C  *** THIS STATEMENT INCORPORATES THE VAR UNIT SUSCEPTANCE
C  *** INTO THE NETWORK ADMITTANCE MATRIX
 810      Y88 = DCMPLX(3.741186,-23.642391) + DCMPLX(0.D0,CSIG)
C  *** 'CSIG' IS THE VAR UNIT SUSCEPTANCE AND IS ASSIGNED TO AN ARRAY
C  *** FOR OUTPUTTING IN THE INTEG PROGRAM.
          X(N+49) = CSIG
       ENDIF

C  *** THIS IS THE END OF THE CONTROL SECTION WHICH DETERMINES THE
C  *** THE VAR UNIT SUSCEPTANCE

C  *** CODE TO IMPROVE CONVERGENCE BY ESTIMATING THE CHANGE
C  *** IN GENERATOR TERMINAL BUS VOLTAGE ANGLE
C  *** IT SEEMS TO SAVE A FEW ITERATIONS

       IF (T .EQ. DT) THEN
          OLDDEL1 = X(2)
          OLDDEL2 = X(9)
          OLDDEL3 = X(16)
       ENDIF

       DELD1 = (X(2) - OLDDEL1)*(180.D0/PI)
       DELD2 = (X(9) - OLDDEL2)*(180.D0/PI)
       DELD3 = (X(16) - OLDDEL3)*(180.D0/PI)
       ANG1 = DATAN2D(X(N+7),X(N+6)) + DELD1
       ANG2 = DATAN2D(X(N+22),X(N+21)) + DELD2
       ANG3 = DATAN2D(X(N+37),X(N+36)) + DELD3
       X(N+6) = CDABS(VOLT1)*DCOSD(ANG1)
       X(N+7) = CDABS(VOLT1)*DSIND(ANG1)
       X(N+21) = CDABS(VOLT2)*DCOSD(ANG2)
```

Figure 31 - continued.

```
      X(N+22) = CDABS(VOLT2)*DSIND(ANG2)
      X(N+36) = CDABS(VOLT3)*DCOSD(ANG3)
      X(N+37) = CDABS(VOLT3)*DSIND(ANG3)


      VOLT1 = DCMPLX(X(N+6),X(N+7))
      VOLT2 = DCMPLX(X(N+21),X(N+22))
      VOLT3 = DCMPLX(X(N+36),X(N+37))


      OLDDEL1 = X(2)
      OLDDEL2 = X(9)
      OLDDEL3 = X(16)

C  *** INFINITE BUS MODULATION CODE

C     EINF = EINFSS + 0.1D0*EINFSS*DSIN((4.33/2.0)*T)
      EINF = EINFSS


C  *** ITERATIVE LOOP TO SOLVE ALGEBRAIC EQUATIONS
C  *** THIS IS WHERE THE SOLUTION OF THE SIDE VARIABLES ACTUALLY BEGINS

      ERR = 1.0
      ITR = 0
      DO WHILE((ERR .GT. 1.D-04) .AND. (ITR .LT. 150))
           DO I=1,40
           XOLD(I) = X(N+I)
           ENDDO
C     ***********************************************************
C     THE FOLLOWING EQUATIONS HAVE THE FORM:
C     VQ = VT_REAL*COS(DELTA) + VT_IMAG*SIN(DELTA)
C     VD = -VT_REAL*SIN(DELTA) + VT_IMAG*COS(DELTA)
C     ***********************************************************

C     X(N+4) = X(N+6)*DCOS(X(2)) + X(N+7)*DSIN(X(2))
C     X(N+5) = -X(N+6)*DSIN(X(2)) + X(N+7)*DCOS(X(2))
      X(N+19) = X(N+21)*DCOS(X(9)) + X(N+22)*DSIN(X(9))
      X(N+20) = -X(N+21)*DSIN(X(9)) + X(N+22)*DCOS(X(9))
      X(N+34) = X(N+36)*DCOS(X(16)) + X(N+37)*DSIN(X(16))
      X(N+35) = -X(N+36)*DSIN(X(16)) + X(N+37)*DCOS(X(16))

C ***** MACHINE IV ALGEBRAIC RELATIONS   ****************
C     THE FOLLOWING ARE EQUATIONS OF THE FORM:
C     ID =( RA(EDP-VD) - XQP(EQP-VQ) )/(RA**2 + XQP*XDP)
C     IQ =( RA(EQP-VQ) + XDP(EDP-VD) )/(RA**2 + XQP*XDP)
C ***********************************************************
C  NOTE THAT EQUATIONS FOR MACHINE #1 HAVE BEEN COMMENTED OUT AS IT
C  IS BEING REPRESENTED AS AN INIFINTE BUS

C     X(N+2) = (RA1*(X(4)-X(N+5))-XQP1*(X(3)-X(N+4)))/
C     &                  ((RA1**2.0)+XDP1*XQP1)
```

Figure 31 – continued.

```
C     X(N+3) = (RA1*(X(3)-X(N+4))+XDP1*(X(4)-X(N+5)))/
C        &                ((RA1**2.0)+XDP1*XQP1)
      X(N+17) = (RA2*(X(11)-X(N+20))-XQP2*(X(10)-X(N+19)))/
      &                ((RA2**2.0)+XDP2*XQP2)
      X(N+18) = (RA2*(X(10)-X(N+19))+XDP2*(X(11)-X(N+20)))/
      &                ((RA2**2.0)+XDP2*XQP2)
      X(N+32) = (RA3*(X(18)-X(N+35))-XQP3*(X(17)-X(N+34)))/
      &                ((RA3**2.0)+XDP3*XQP3)
      X(N+33) = (RA3*(X(17)-X(N+34))+XDP3*(X(18)-X(N+35)))/
      &                ((RA3**2.0)+XDP3*XQP3)


C     ************** AXIS TRANSFORMATION *******************
C         ID AND IQ TO REAL AND IMAGINARY TERMINAL CURRENTS
C     X(N+8) = X(N+3)*DCOS(X(2)) - X(N+2)*DSIN(X(2))
C     X(N+9) = X(N+3)*DSIN(X(2)) + X(N+2)*DCOS(X(2))
      X(N+23) = X(N+18)*DCOS(X(9)) - X(N+17)*DSIN(X(9))
      X(N+24) = X(N+18)*DSIN(X(9)) + X(N+17)*DCOS(X(9))
      X(N+38) = X(N+33)*DCOS(X(16)) - X(N+32)*DSIN(X(16))
      X(N+39) = X(N+33)*DSIN(X(16)) + X(N+32)*DCOS(X(16))


C     CUR1 = DCMPLX(X(N+8),X(N+9))
C     ***** FOR INFINITE BUS SIMULATION  ******
      CUR1 = (EINF - VOLT1)/IMPED1
      CUR2 = DCMPLX(X(N+23),X(N+24))
      CUR3 = DCMPLX(X(N+38),X(N+39))


C     *** THIS INNER LOOP REDUCES THE OVERALL NUMBER OF ITERATIONS
C     *** REQUIRED BY APPROXIMATELY ONE HALF
          DO K = 1,6

              VOLT4 = -(Y14*VOLT1 + Y45*VOLT5 + Y46*VOLT6)/Y44
              VOLT5 = -(Y45*VOLT4 + Y57*VOLT7)/Y55
              VOLT6 = -(Y46*VOLT4 + Y69*VOLT9)/Y66
              VOLT7 = -(Y27*VOLT2 + Y57*VOLT5 + Y78*VOLT8)/Y77
              VOLT8 = -(Y78*VOLT7 + Y89*VOLT9)/Y88
              VOLT9 = -(Y39*VOLT3 + Y69*VOLT6  + Y89*VOLT8)/Y99


          ENDDO
C     *** THIS IS THE END OF THE 'INNER' LOOP ***

      VOLT1 = (CUR1 - Y14*VOLT4)/Y11
      VOLT2 = (CUR2 - Y27*VOLT7)/Y22
      VOLT3 = (CUR3 - Y39*VOLT9)/Y33


C     *** SEPARATE REAL AND IMAGINARY VOLTAGE COMPONENTS ****
      X(N+6) = DREAL(VOLT1)
      X(N+7) = DIMAG(VOLT1)
      X(N+21) = DREAL(VOLT2)
      X(N+22) = DIMAG(VOLT2)
```

Figure 31 - continued.

```
      X(N+36) = DREAL(VOLT3)
      X(N+37) = DIMAG(VOLT3)


C  ******* MACHINE ELECTRICAL POWER OUT ***********************
C     EQUATIONS FOR ELECTRICAL POWER GENERATED
C     PE = VD*ID + VQ*IQ
C  ***********************************************************
      X(N+1) = X(N+5)*X(N+2) + X(N+4)*X(N+3)
      X(N+16) = X(N+20)*X(N+17) + X(N+19)*X(N+18)
      X(N+31) = X(N+35)*X(N+32) + X(N+34)*X(N+33)


C  *** THIS SECTION CALCULATES ERRORS,COUNTS ITERATIONS
C  *** AND DETERMINES WHEN THE MAIN LOOP IS EXITED.


      ERR = 0.00
      ITR = ITR + 1
      IF (ITR .GT. 149) PRINT*,'WARNING !!! *** NOT CONVERGING !!! *** '
         DO I=1,40
         IF (ABS(X(N+I)) .GT. 1.D-04) THEN
            DIFF(I) = ABS(XOLD(I) - X(N+I))/ABS(X(N+I))
            ELSE
            DIFF(I) = ABS(XOLD(I) - X(N+I))
         ENDIF
         IF (DIFF(I) .GT. ERR) THEN
             ERR = DIFF(I)
C            PRINT *,'ITR =',ITR,' ERR=',ERR,' NO =',N+I
         ENDIF
         ENDDO
      ENDDO
C  *** END OF MAIN LOOP TO SOLVE ALGEBRAIC RELATIONS  ***


C  *** EXCITER SATURATION EQUATIONS (VT,V1,SE)
C  *** MACHINE 2
      X(N+29) = (X(N+19)**2 + X(N+20)**2)**.5
      IF (X(13) .LE. 0.75*EFMX2) THEN
          K12 = 4.0*SE75MX2/(3.0*EFMX2)
          K22 = 0.0
      ELSE
          K12 = 4.0*(SEMX2 - SE75MX2)/EFMX2
          K22 = 4.0*SE75MX2 - 3.0*SEMX2
      ENDIF
      X(N+27) = X(13)*(K12*X(13) - K22)


C  *** MACHINE 3
      X(N+44) = (X(N+34)**2 + X(N+35)**2)**.5
      IF (X(20) .LE. 0.75*EFMX3) THEN
          K13 = 4.0*SE75MX3/(3.0*EFMX3)
          K23 = 0.0
      ELSE
```

Figure 31 - continued.

```
            K13 = 4.0*(SEMX3 - SE75MX3)/EFMX3
            K23 = 4.0*SE75MX3 - 3.0*SEMX3
        ENDIF
        X(N+35) = X(20)*(K13*X(20) - K23)

C  ***  AMPLIFIER SATURATION
C  ***  MACHINE 2

        IF(X(12).GT.1.0)THEN
            X(12) = 1.0
        ELSEIF(X(12).LT.-1.0)THEN
            X(12) = -1.0
        ENDIF

C  ***  MACHINE 3

        IF(X(19).GT.1.0)THEN
            X(19) = 1.0
        ELSEIF(X(19).LT.-1.0)THEN
            X(19) = -1.0
        ENDIF

C ************ END OF EXCITER SECTION  ********************

C     PRINT*,'T =',T,'   ITR = ',ITR,'ERR =',ERR
C ******* CALCULATE ROTOR ANGLES IN RADIANS
        ANG8 = DATAN2(DIMAG(VOLT8),DREAL(VOLT8))
        X(N+46) = 180.0*X(2)/PI
        X(N+47) = 180.0*X(9)/PI
        X(N+48) = 180.0*X(16)/PI
        IF (X(N+48) .GT. 150.0) THEN
            PRINT *,'  SYSTEM UNSTABLE --- RUN ABORTED 2MIED '
            STOP
        ENDIF

C     WRITE(*,809) T,ATAN2D(X(N+22),X(N+21)),ITR
C 809 FORMAT( ' ACT ',PE11.4,1PE14.7,'PRE ITR=',I4)

        IF( DT .GT. 0.D0) THEN
            TOTCYC = TOTCYC + 1.0
            TOTITR = TOTITR + ITR
        ENDIF

        IF(TICK2 .EQ. 1) THEN
            AVGITR = TOTITR/TOTCYC
            TOTITR = 0.D0
            TOTCYC = 0.D0
            WRITE(*,990) T,AVGITR
 990        FORMAT(' TIME =',1PE11.4,2X,'  AVG ITR =',1PE11.4)
```

Figure 31 -   continued.

```
      ENDIF

C *** THIS IS SOME CODE WHICH CAN BE USED TO LOOK AT VOLTAGE MAGNITUDES
C *** IN THE NETWORK AS THE SIMULATION IS GOING ON

      IF (TICK .EQ. 1) THEN
C        WRITE(17,900) T,CDABS(VOLT2),CDABS(VOLT3),CDABS(VOLT7),
C     &                     CDABS(VOLT8),CDABS(VOLT9)
C        WRITE(17,900) T,X(N+50),X(23),CDABS(VOLT8),ANG8
C 900    FORMAT(6(1X,1PE11.4))
      ENDIF

      RETURN
      END
```

Figure 31 – continued.

APPENDIX B

PROGRAM FOR CALCULATING INITIAL CONDITIONS